Surface charge and equilibration of calcite with CO_2 gas in granitic groundwaters

Master's thesis

University of Helsinki

Faculty of Science

Department of Chemistry

Artem Dziuba

6.11.2023

HELSINGIN YLIOPISTO
HELSINGFORS UNIVERSITET
UNIVERSITY OF HELSINKI
MATEMAATTIS-LUONNONTIETEELLINEN TIEDEKUNTA
MATEMATISK-NATURVETENSKAPLIGA FAKULTETEN
FACULTY OF SCIENCE

Tiedekunta – Fakultet – Faculty Faculty of Science		Koulutusohjelma – Utbildningsprogram – Degree programme Master's Programme in Chemistry and Molecular Sciences
Opintosuunta – Studieinrikting – Study track Radiochemistry		
Tekijä – Författare – Author Artem Dziuba		
Työn nimi – Arbetets titel – Title Surface charge and equilibration of calcite with CO_2 gas in granitic groundwaters		
Työn laji – Arbetets art – Level Master's Thesis	Aika – Datum – Month and year 11/2023	Sivumäärä – Sidoantal – Number of pages 78

Tiivistelmä – Referat – Abstract

Surface charging behavior of commercial pure calcite and calcite samples from the Bukov underground research facility was studied by measuring the zeta potential of the samples after equilibration with CO_2 gas and determining their cation exchange capacity.

For zeta potential measurements, different calcite samples with grain sizes under 25 µm were submerged into five different electrolyte solutions: 0.01 M NaCl, 0.001 M $CaCl_2$, 0.005 M NaCl + 0.0025 M $MgCl_2$, 0.0025 M NaCl + 0.00375 M $MgCl_2$, and a synthetic groundwater simulant (SGW2). A pH range of 6.5 – 11 was established and maintained across sample series for the duration of the experiments, and the samples were equilibrated with CO_2 gas by regular bubbling of a 250 ppm CO_2/N_2 gas mixture into the solutions in 1-hour sessions. The length of the equilibration process varied from three days to one month, and after its conclusion the zeta potential of each sample was measured. The goal of the experiments was to evaluate the feasibility of equilibrating calcite samples with CO_2 when studying their zeta potential. Additional goals included comparing different types of calcite in different solutions, as well as determining an optimal duration for equilibration. The results were compared with an earlier study where calcite zeta potential was determined under total CO_2 exclusion.

For the determination of cation exchange capacity, two cobalt hexamine trichloride solutions were used, one saturated with pure calcite and one saturated with Bukov calcite. Samples of both types of calcite were shaken for 1 hour in their respective solutions, and the ionic composition of the supernatant from each sample was determined using microwave plasma atomic emission spectrometry. Cation exchange capacity was calculated from the measurement results.

According to the results obtained, long-term exposure and equilibration with CO_2 may have a positive effect on the internal stability of calcite samples and lead to more reliable zeta potential measurements. Samples showed minimal fluctuation in the concentration of Ca in bulk solution after one week of equilibration, and no significant rise or decline in stability was noted to occur if equilibration was continued beyond one week. Compared to CO_2 exclusion, equilibration produced more consistent trends in zeta potential values, though the results were heavily dependent on the electrolyte solution used in the experiment. Cation exchange capacity experiments also produced much larger values than the previous exclusion study despite using the same types of sample, hinting at a significant difference in the grain sizes used.

Avainsanat – Nyckelord – Keywords

Calcite, zeta potential, surface charge, equilibration

Säilytyspaikka – Förvaringställe – Where deposited
E-thesis

Muita tietoja – Övriga uppgifter – Additional information

Contents

1. Introduction

Spent nuclear fuel (SNF) presents a unique challenge to operating a nuclear power plant. Nuclear fuel is initially fabricated from natural uranium ore containing ^{235}U, ^{238}U and their daughter radionuclides. During the operation of a power plant nuclei of ^{235}U in nuclear fuel undergo fission, splitting into two fission products and increasing the overall radioactivity of the fuel in the process [1]. The fission of ^{235}U also releases neutrons, which can in turn strike other ^{235}U nuclei and induce further fission, sustaining the process in a chain reaction. Most of the fission products created in this way have very short half-lives and quickly decay away, but certain long-lived radionuclides are created as well. Over time, the fissile fraction of the fuel gradually decreases until it can no longer support a self-sustaining chain reaction and the fuel becomes spent. However, even after the fuel is no longer feasible to use for power generation, it cannot simply be discarded as it remains dangerously radioactive due to the presence of various daughter radionuclides created during its use.

After discharge from a reactor, the radiation intensity and decay heat of the fuel are so great that it must initially be stored under water to cool down before transport and storage can even be considered [2]. Yet even after the heat and radiation decrease sufficiently for the spent fuel to be moved, it still poses a significant risk for a considerable length of time. Certain shorter-lived radionuclides contained in the fuel still take hundreds of years to decay to safe levels, and it takes thousands more years for the long-lived components to decay until the fuel is no more dangerous than the natural uranium ore from which it originally came [1, 2]. During this time the fuel emits highly penetrating radiation capable of giving a lethal dose to any living organisms nearby, and while the danger decreases over time, protective measures are still required in the vicinity of the spent fuel for hundreds of years. In addition to external radiation, internal radiation also poses a threat if radioactive substances released from the fuel are accidentally inhaled or ingested. In this case, the radiation is no longer limited by its penetrating power as it may be emitted inside an organism [1, 3]. As such, while SNF is no longer of any practical use to a nuclear power plant operator, it is a considerable radiotoxicity hazard for any living organisms in its vicinity and remains as such for an extremely long time, requiring special care and unique measures to be taken in its disposal.

Given how hazardous spent nuclear fuel is and for how long it retains its hazardous properties, the most effective way to manage the risk it poses is to reduce the probability of exposure of living organisms to SNF [1]. Ideally, SNF would be completely isolated from the living environment until it

no longer posed a threat, staying reliably contained and undisturbed in the long timeframe dictated by the decay of its components. SKB in Sweden and Posiva in Finland have developed a method of disposal that can meet these requirements: the KBS-3 method, which relies on a series of natural and artificial barriers [4–6]. In this method, SNF is stored deep underground in gas-tight and water-tight copper-iron canisters, which are placed into deposition holes drilled into the floors of deposition tunnels (Figure 1). A swelling clay buffer material surrounds the canisters, separating them from the bedrock, and in the last stage, all access tunnels and underground openings are to be filled using materials with low permeability. Spent nuclear fuel is thus isolated from the living environment first by its canister, followed by the layer of buffer material, the filled-in tunnels, the surrounding bedrock and finally the sealed openings (Figure 2). In this way, SNF is rendered inaccessible to any living beings that otherwise may have accidentally become exposed to radiation while the fuel decays. The depth of the repository ensures adequate attenuation of external radiation, while the risk of internal radiation is effectively eliminated as the spent fuel is contained behind multiple barriers designed with redundancy in mind. Even in the event of the canisters becoming damaged, the number of additional barriers as well as the sheer quantity of rock surrounding the canisters due to the depth is meant to prevent radionuclides from reaching the surface and ensure complete long-term isolation.

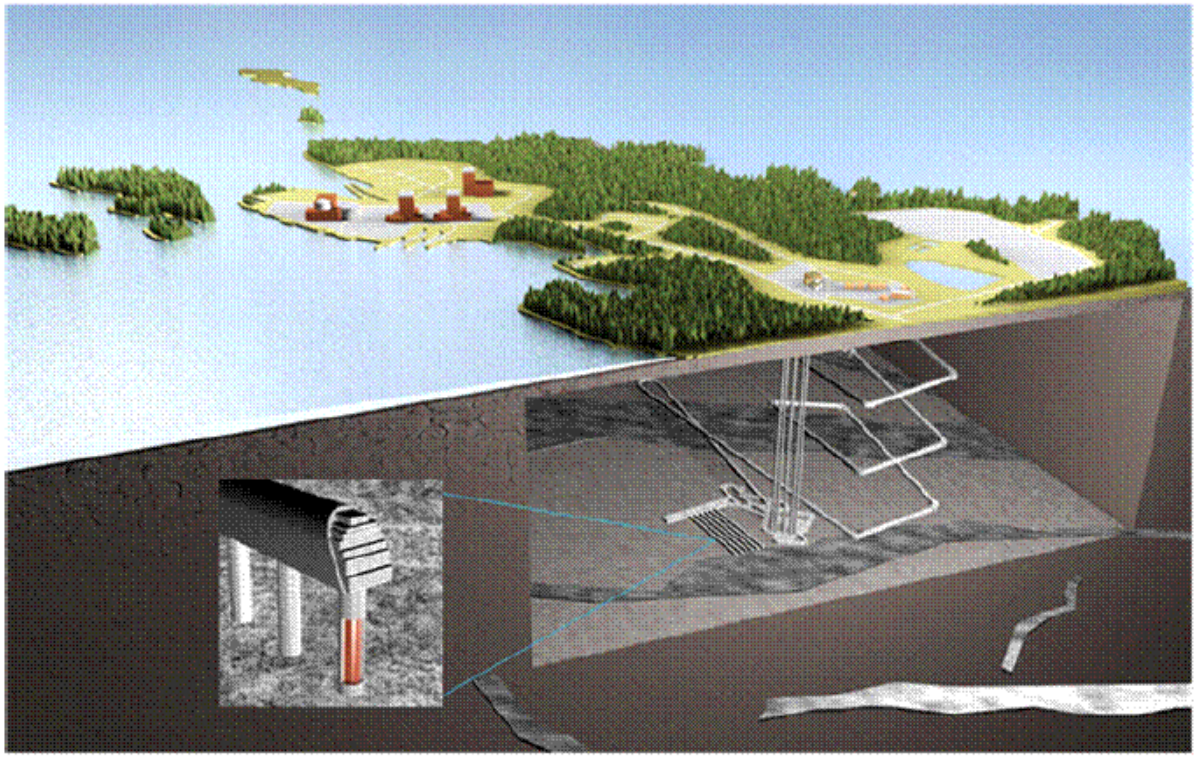

Figure 1. Overview of the KBS-3V (vertical) design [4].

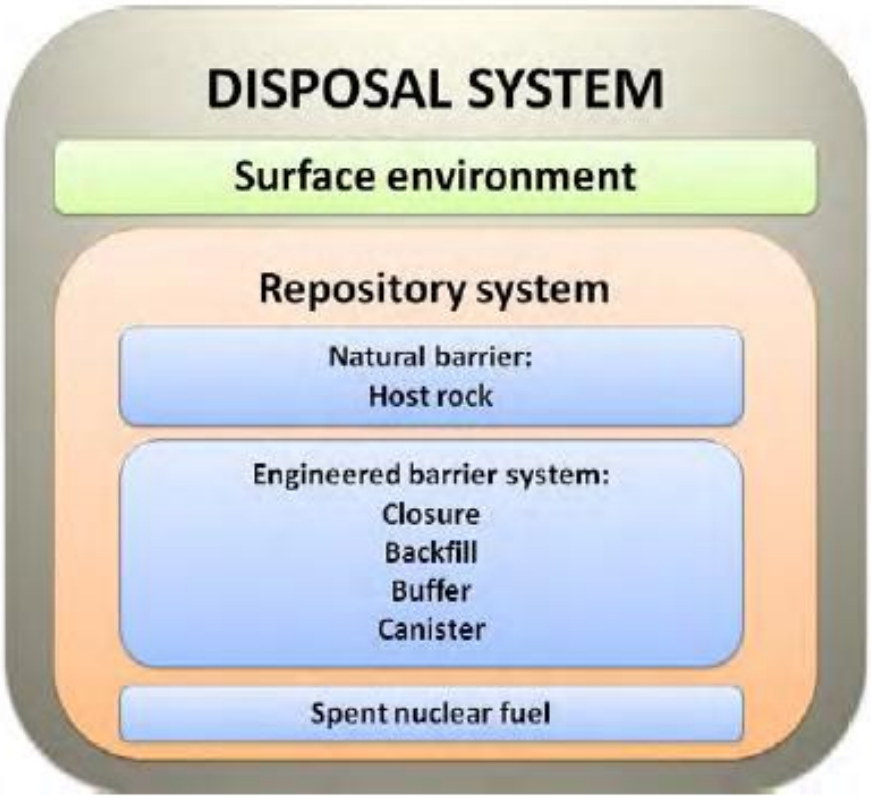

Figure 2. Summary of the KBS-3 method [5].

Ideally, the canisters alone would be sufficient to contain the spent nuclear fuel for the entire duration of its decay, but considering the extremely long timeframe involved, many unforeseen events could occur despite their low probability and any precautions taken. Initial canister defects that go unnoticed or their corrosion over time, rock shear and higher groundwater flow rates than predicted could all impact the performance of the canister and lead to the release of radionuclides [4, 7]. In this case, the host rock barrier surrounding the canister would be of particular importance. While the primary role of the rock barrier is to physically separate the spent nuclear fuel from the surface and provide stable, predictable conditions for storage, it could also retain liberated radionuclides by sorption onto fraction minerals. Radionuclide mobility would thus be reduced, ensuring they remain contained even if they pass the initial barrier. Retention in crystalline rock and rock minerals could therefore prevent many escaped radionuclides from reaching the biosphere in the event of other barriers failing [8–14].

A particularly noteworthy mineral in this regard is the carbonate mineral calcite ($CaCO_3$). Calcite is one of the most common and widespread carbonate minerals in the Earth's crust, generally occurring in sedimentary rocks and ranging anywhere from tropical environments to glacial settings

[15, 16]. Calcite-containing sedimentary rocks account for around 20% of all surface sedimentary rocks, with calcite itself making up about 4% of the Earth's crust [17, 18]. It is the principal mineral in certain metamorphic rocks, such as marble and calcareous gneiss as well as limestone. Limestone in particular primarily consists of shells of dead marine organisms, for which calcite is an important biomineral, acting as the primary constituent of their shells and skeletons along with other carbonates like aragonite and magnesian calcite [19–21]. Due to their role as skeletal minerals, these carbonates are biologically mediated, and the formation and exact composition of carbonate sediments is closely tied to the local biota [17]. As such, the marine environment is a major source of calcite deposits, with numerous different organisms precipitating calcium carbonate as organic compounds from microbes, as skeletal components of animals, and as byproducts of animal metabolic activity, in addition to direct precipitation of calcium carbonate out of water. Most commonly this occurs in shallow marine settings, but calcite sediments are also found in oceans, freshwater lakes, streams, calcareous soils and caves, with the oldest sedimentary rocks formed in this way dating back billions of years [17, 22]. Different physical, chemical and biological influences during sediment formation also affect the crystal morphology of the resulting mineral, resulting in a great variety of possible crystal forms [16, 17]. As a result, calcite sediments are found in many different environments around the world and are highly diverse, reflecting the environments in which they originally formed and being active participants in their chemical and biological processes.

Carbonate minerals are known to be highly reactive in terms of dissolution and precipitation processes, and given its level of interaction with its local environment, calcite is no exception [15, 23, 24]. Groundwaters are often in contact with carbonate minerals as they flow, of which calcite is the most abundant. As its dissolution and precipitation reactions are quick relative to most groundwater flow rates, groundwaters tend to become saturated with calcite. In addition to dissolution and precipitation, it has also been shown that carbonate minerals are actively involved in sorption processes involving trace elements [24, 25]. As such, dissolved calcite particles may play an important role in slowing the migration of divalent metal ions in groundwater. This property also extends to radioactive substances, such as ^{226}Ra: a long-lived radionuclide that is a part of the natural decay chain of uranium. In the context of spent nuclear fuel disposal, calcite may therefore be able to reduce the mobility of escaped radionuclides via sorption and prove to be an important part of the natural rock barrier, acting as a sink for both conventional and radioactive contaminants [7, 18, 24, 26–29].

Calcite is present in notable quantities at Olkiluoto: a site that was proposed as a potential repository for spent nuclear fuel with the KBS-3 design. The bedrock within the site contains networks of fractures and fracture zones, which act as dominant paths for groundwater flow and are coated or filled with various minerals, with calcite being one of the most prevalent [3]. This creates the exact conditions in which groundwaters may become saturated with calcite, and given the plans for long-term storage of spent nuclear fuel at the site, there is a possibility of these groundwaters interacting with escaped radionuclides. As such, this potential interaction warrants further investigation to better understand the role calcite may have in restricting radionuclide migration, especially considering the widespread nature of calcite and its likely occurrence at other potential disposal sites.

The goal of this study was the determination of calcite surface charge following a period of equilibration with different electrolyte solutions and CO_2 gas. In addition, the effect of different solution conditions on calcite surface charge was investigated by using a groundwater simulant and several solutions containing individual ionic compounds found in groundwaters. By gaining a greater understanding of surface charge and the interactions on the interface between the calcite mineral lattice and the bulk solution, calcite's efficacy in the retardation of escaped radionuclides could be evaluated more effectively [15, 24, 27, 28]. In this work, two different kinds of calcite (samples from the Bukov research facility [30] and commercial pure calcite) were equilibrated with CO_2 gas in different electrolyte solutions and a groundwater simulant, after which the zeta potentials of the calcites were measured as a means of studying surface charging behavior. Calcite CEC was also determined using the cobalt hexamine trichloride method [31]. The equilibration process was monitored by taking aliquots for measurement with MP-AES to track Ca concentration, while zeta potentials were measured using a Malvern Zetasizer Nano device.

2. Theoretical background

2.1 Zeta potential

Zeta potential is a parameter used to describe charging behavior at various phase interfaces, such as solid-liquid, liquid-liquid and liquid-gas. This work was mainly concerned with the solid-liquid interface. When in contact with an aqueous solution, a solid surface gains an electric charge. Oppositely charged ions present in the aqueous phase attempt to compensate this surface charge,

creating two distinct layers of ions. This is known as the electrochemical double layer model. Close to the solid surface is a stationary immobile layer of ions that counteract its charge, and further away is a diffuse mobile layer of counterions that are less strongly attracted to the surface. Beyond the diffuse layer, ions experience effectively no attraction to the solid and are free as part of the bulk solution. The existence of a surface charge thus creates a surface potential that decays as a function of distance from the solid surface. The potential outside of the stationary layer, right on the boundary between the stationary and diffuse layers, is defined as the zeta potential [32].

Surface charge is primarily formed by two mechanisms: acid-base reactions between surface functional groups and the aqueous solution, and adsorption of ions onto the solid surface. Acidic groups, such as carboxylic acids and hydroxyls, dissociate in solution and assume a negative charge, while basic groups like amines become protonated and acquire a positive charge (Figure 3). When bound to a solid surface, these functional groups react with the aqueous solution in their characteristic manner and thus generate a net surface charge. The outcome of this process is greatly influenced by the area density of the surface functional groups and the solution pH. Dissociation/protonation reactions may be inhibited at high group densities due to electrostatic repulsion between neighboring groups, while pH will either enhance or suppress these reactions depending on the concentration of available H^+. Zeta potential is therefore highly dependent on the type and number of functional groups on the solid surface, which in turn are influenced by pH [32].

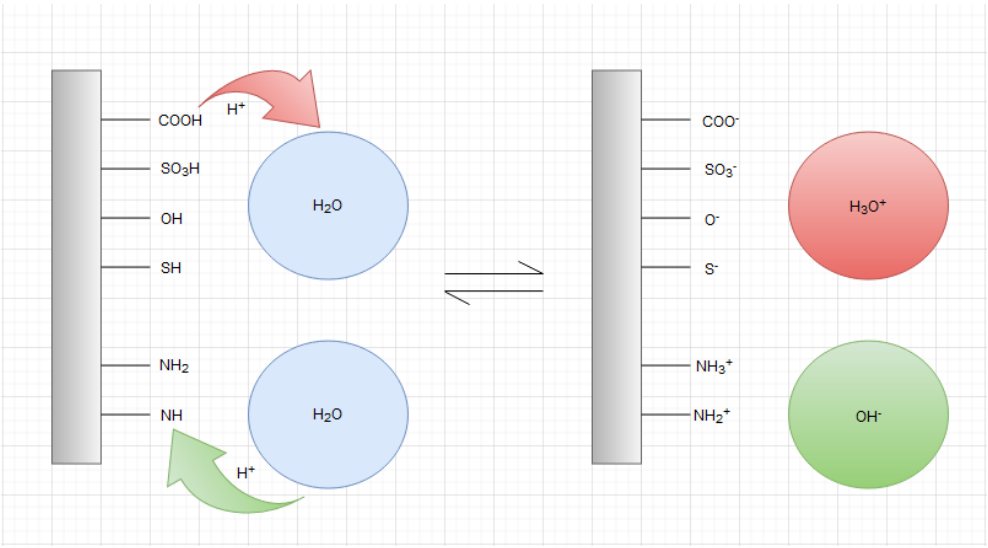

Figure 3. Formation of surface charge by acid-base reactions.

For surfaces without functional groups, surface charge and zeta potential are still observable due to ion adsorption. Surfaces that lack functional groups behave hydrophobically in solution. As a result,

the adsorption of ions such as OH^- and H_3O^+ is preferential to that of water molecules, leading to the replacement of water molecules on the solid surface by water ions and the subsequent formation of a surface charge (Figure 4). The exact mechanism by which this process occurs is not yet fully understood, but pH is known to still have an important role as it directly denotes the concentration of OH^- and H_3O^+ and ultimately determines the type and number of ions available for adsorption to the surface [32].

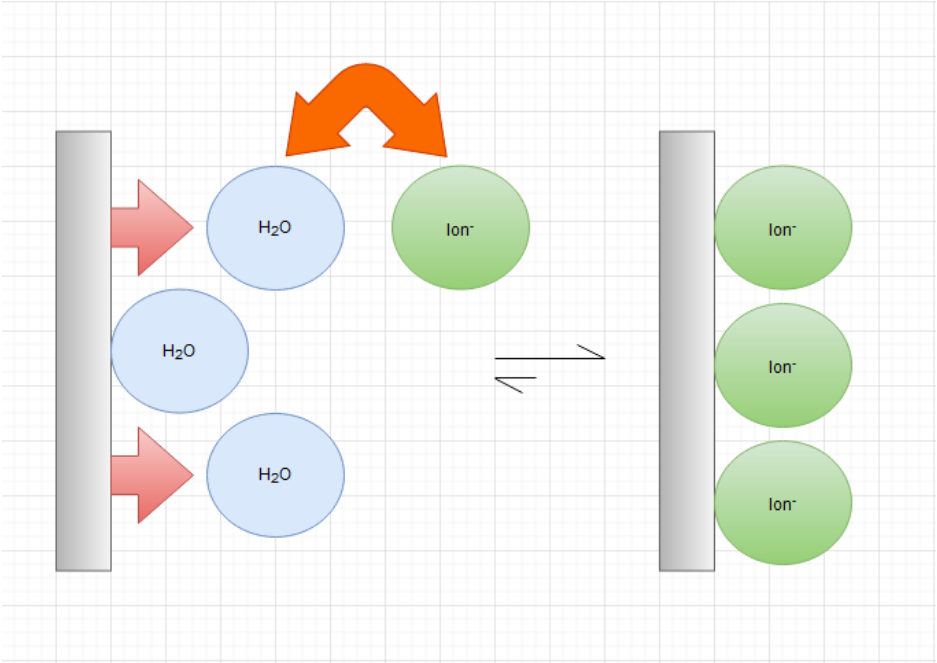

Figure 4. Formation of surface charge by ion adsorption.

While pH is the most important parameter of the liquid phase, zeta potential is also influenced by several other factors, such as the ionic strength of the solution, porosity of the solid, temperature and measurement time. Ionic strength is especially noteworthy because at high electrolyte concentrations the magnitude of zeta potential tends to decrease. This effect is even stronger in the presence of more complex solutes like $CaCl_2$ and Na_2SO_4, owing to the specific adsorption and complexation of divalent ions on the surface. At high ionic strengths, for example, it is possible for negatively charged surface groups to be occupied in complexes to the point that the surface becomes neutral or even positively charged [32]. It is therefore crucial to consider the composition and concentration of the aqueous phase when measuring and interpreting zeta potentials as the results are heavily dependent on the chemistry of the solution.

One final factor to consider in the scope of this work is the effect of CO_2. Preferential adsorption of CO_2 may occur on hydrophobic surfaces, causing changes in zeta potential [32]. The solid surface

may also adsorb CO_3^{2-}, while the dissolution of CO_2 and formation of carbonic acid can alter the pH of the solution [15]. All these phenomena combined mean that the dissolution of CO_2 from air can significantly alter the measured zeta potential so it no longer reflects the interactions between only the solid and the original aqueous solution. One proposed method to counteract this is to purge the solution with N_2 [32, 33]. However, CO_2 dissolution resumes quickly if the N_2 flow is stopped, making it necessary for the purge to be continuous. An alternative approach is to expose the samples to a constant pCO_2, allowing CO_2 to dissolve and saturate them quantitatively, which makes it possible to tie zeta potential results to specific conditions [18]. Ideally, this would be achieved in a closed system with its own atmosphere where samples are allowed to interact and equilibrate with the surrounding gas phase, but this approach is extremely slow. Instead, a faster and more direct way was attempted in this work, discussed in detail in Section 3.3.

2.2 Measurement of zeta potential

A Malvern Instruments Zetasizer Nano particle analyzer was used in this work to measure zeta potentials (Figure 5). The device performs an electrophoresis experiment on sample particles and measures their velocity using Laser Doppler Velocimetry. Having determined the electrophoretic mobility, it then applies the Henry equation to obtain the zeta potential [34].

The basis of the Zetasizer's operation lies in the electrochemical double layer model. The diffuse layer of counterions has a boundary beyond which ions are effectively free. Within this boundary, however, ions experience enough attraction to the charged solid surface that, as a particle moves, they travel with it as one stable entity. When an electric field is applied across an electrolyte, any such charged particles will be attracted to the electrode of opposite charge. Particle movement will be opposed by viscous forces acting upon them until an equilibrium is reached and their velocity becomes constant. Velocity in this context is the same as electrophoretic mobility, which can be used to calculate the zeta potential from the Henry equation [34]:

$$U_E = \frac{2\varepsilon z f(ka)}{3\eta} \quad (1)$$

where U_E is electrophoretic mobility, η is viscosity, ε is the dielectric constant, f(Ka) is Henry's function and z is the zeta potential. U_E is obtained through Laser Doppler Velocimetry. A potential is applied to a cell with two electrodes at either end, causing charged particles to move (Figure 6).

Light scattered from these particles at an angle of 17° is combined with a reference beam to produce a fluctuating intensity signal. The rate of fluctuation is proportional to the speed of the particles and thus their electrophoretic mobility [34].

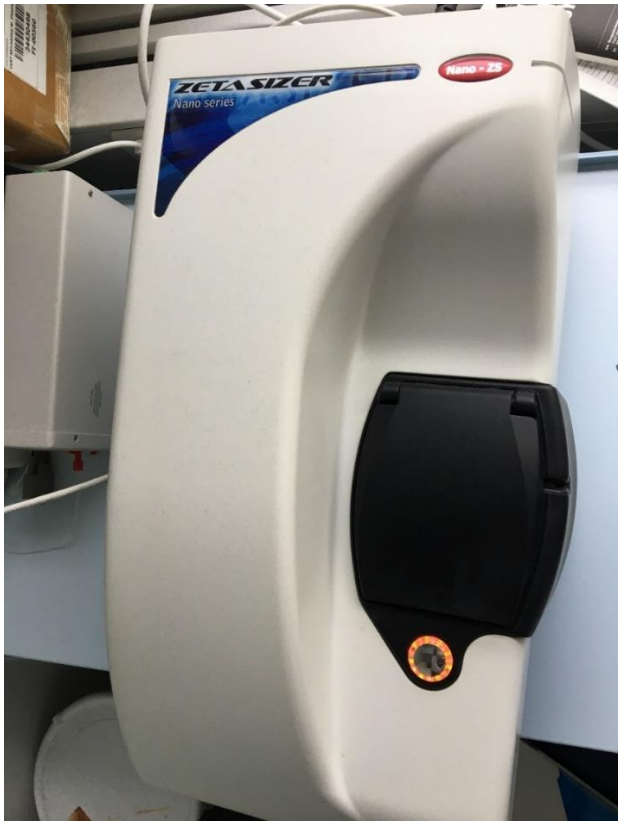

Figure 5. The Zetasizer Nano device used in this work.

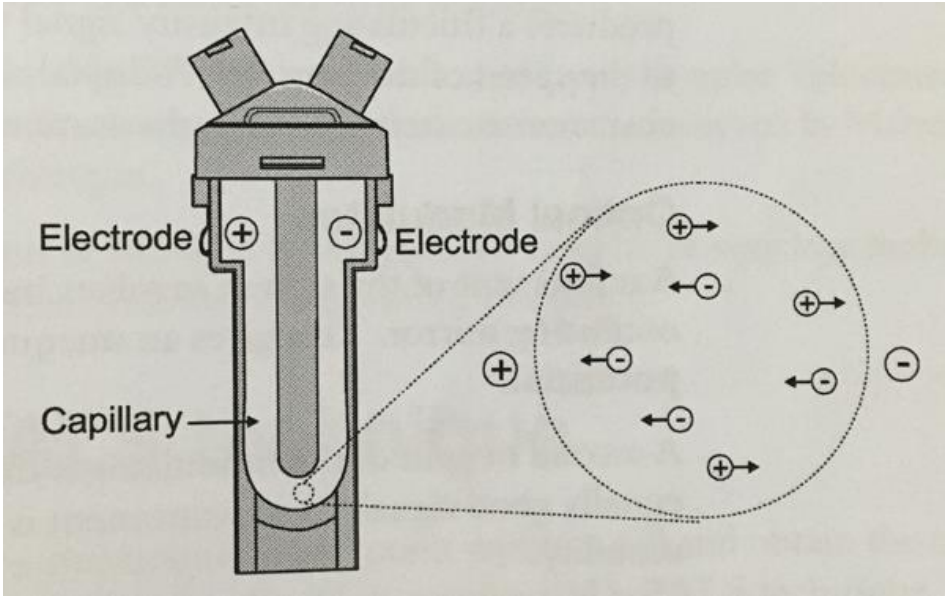

Figure 6. The principle of zeta potential measurement through electrophoretic mobility [34].

2.3 Calcite

The ability of mineral particles in natural waters to react with dissolved substances depends on numerous properties, such as specific surface area, cation exchange capacity, surface hydrophobicity/hydrophilicity and surface charge [35]. In this work, emphasis was placed on surface charge. The mechanisms for its formation are different for different minerals, but in the case of carbonates, surface charge arises mainly from hydrolysis and complex formation reactions involving surface ions. Upon contact of calcite with water, the terminated outermost calcite surface becomes hydrolyzed with a layer of H and OH to counteract charge imbalances, forming two types of surface site: >CaOH and >CO_3H [36–38]. These sites undergo further reactions with Ca^{2+}, CO_3^{2-}, HCO_3^-, $CaHCO_3^+$, H^+ and OH^- present in solution (Figure 7). Calcite surface charge therefore depends on the distribution of Ca^{2+} and different carbonate ion species (potential-determining ions) between the mineral surface and solution [15, 39, 40]. H^+ and OH^- do not affect electrokinetic potential directly and instead regulate the speciation of carbonate ions. As such, the study of calcite surface charge primarily involves dissolved Ca^{2+} and carbonate species.

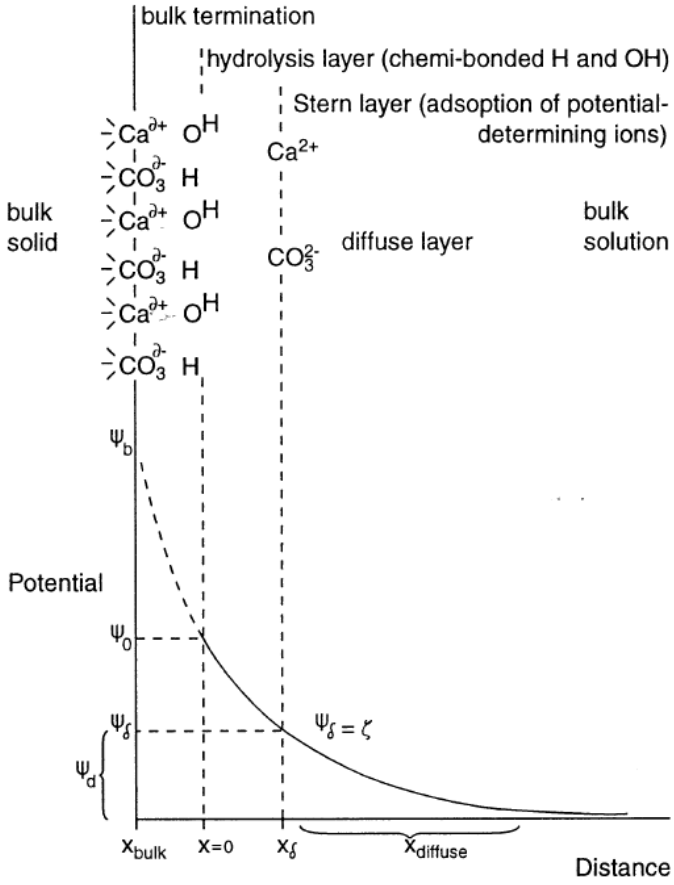

Figure 7. Electrical double layer model for calcite surface in contact with an aqueous solution [37].

Net surface charge depends on the relative amounts of potential-determining ions adsorbed to the calcite surface. In the pH range up to 6.5, the dominant carbonate species in solution are dissolved molecular CO_2 and undissociated H_2CO_3; between pH 6.5 and 10 it is HCO_3^-; above pH 10 the dominant species is the anion CO_3^{2-}. In theory, as anionic species become more prevalent at higher pH than the positively charged Ca^{2+} , with rising pH the surface should become more populated with adsorbed anions and its potential should thus become increasingly negative [33, 35, 40]. The trend with pH is not entirely clear, however, as at lower pH values calcite dissolution begins to occur, leading to the detachment of constituent ions from the surface and overall decrease in surface potential. This could be caused by several factors, such as higher loss of CaOH than CO_3H, specific adsorption of anions or decrease in the surface area of calcite grains [35]. Surface chemistry is further complicated at all pH values if contaminants are present. Nevertheless, it is clear that calcite's ability to adsorb contaminants depends on the surface charge it exhibits, which in turn is heavily dependent on the pH of the solution in which it is placed.

Another important factor to consider with zeta potentials is whether the calcite and solution have reached equilibrium [18, 35, 38]. Given the importance of dissolved Ca^{2+} and carbonate species to zeta potential, their amount in solution should remain constant for surface reactions to reach completion – otherwise the surface charge will constantly change along with ongoing surface chemistry, rendering any measurements unreliable [15, 39, 40]. For this reason, it is crucial to ensure equilibrium is achieved between calcite, solution and surrounding gas phase to prevent the addition of potential-determining ions to the system, such as increasing the amount of Ca^{2+} through dissolution of calcite or carbonates entering the solution as CO_2 from the atmosphere. As such, the goal of this work was to study the surface charges of calcite samples following an equilibration period with CO_2 gas. By doing so, the amount of carbonates in solution would ideally maintain a constant level, while their speciation would be controlled by adjusting solution pH. In turn, Ca^{2+} would be monitored by measuring the elemental composition of equilibration solutions until its concentration stabilizes, accounting for all relevant potential-determining ions.

2.4 Determination of the elemental composition of samples

In order to follow solution conditions and evaluate the effectiveness of equilibration, a microwave plasma atomic emission spectrometer (MP-AES) was utilized in this work. This measurement technique is based on the ability of atoms to be excited to higher-energy states and subsequently relax, whereupon they emit their excess energy as light. Atoms of different elements have a

characteristic wavelength at which they emit this light, creating a specific emission spectrum depending on what elements are present in the sample. By measuring the wavelengths and their intensities, the elemental composition of a sample can be studied and quantified [41].

MP-AES accepts only liquid samples, which are introduced into the instrument as a fine mist using a nebulizer. The nebulizer selects the smallest particles available and directs them into the plasma. The high-temperature plasma is needed to dry, atomize and excite sample atoms, which proceed to relax and emit light. Depending on the analysis being performed, specific wavelengths of light can be selected for detection to provide data on specific elements. The intensity of each emitted line in the spectrum is directly proportional to the concentration of its corresponding element, allowing the MP-AES to calculate the concentration of each individual element in a sample by comparing measurement results to standard samples with a known concentration [41, 42].

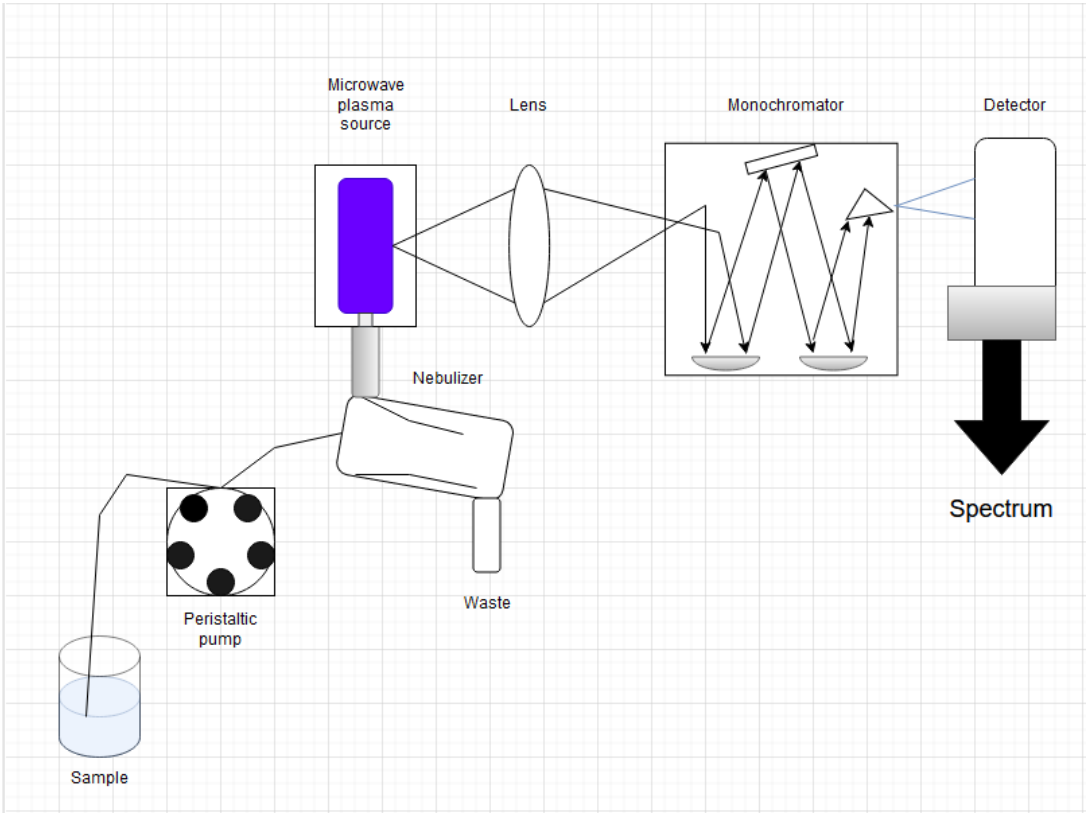

Figure 8. The principle of MP-AES operation.

The biggest difference between MP-AES and comparable analytical techniques comes from the way it generates its plasma. Prior to the introduction of MP-AES, inductively coupled plasma had already been used for the purposes of atomization and excitation in techniques such as ICP-MS and ICP-AES [42]. Both are highly useful and reliable techniques, but their operation is costly as the plasma requires a continuous supply of expensive argon gas. Alternative microwave-based plasma sources

had also been previously developed, being able to use less expensive gases and in smaller quantities. However, these showed significantly worse performance characteristics compared to ICP techniques and were much more demanding in terms of sample introduction. As a result, microwave plasma did not gain popularity until an alternative way to generate it by coupling energy from the magnetic field was developed [43]. This change improved the microwave plasma technique to the point where its performance began to approach that of ICP, albeit still falling short in various aspects like sensitivity, detection limits and spectral interferences [43, 44].

Nevertheless, MP-AES makes up for its shortcomings by offering other advantages, most prominently in operating costs, size and safety [43, 44]. It is much cheaper to operate due to using nitrogen from a nitrogen generator as its plasma support gas, which also removes the need to handle gas cylinders. A more compact size also makes the instrument more versatile and easier to accommodate in a laboratory setting. Due to these advantages and solid performance, MP-AES is a suitable alternative for more routine analyses that do not necessarily require the level of precision offered by ICP.

Figure 9. The MP-AES device used in this work.

2.5 Cation exchange capacity

Negative charges on the surface of soils and minerals can arise for a variety of reasons, such as the dissociation of acidic functional groups or the existence of non-compensated bonds. These sites are able to reversibly retain cations from the environment through electrostatic interactions, which is the foundation for a soil's ability to maintain stocks of nutrients and other charged species. A way to quantify this ability is to determine a soil's cation exchange capacity (CEC), defined as a measure of the quantity of negatively charged sites on soil surfaces [45, 46]. As such, CEC is a useful indicator of how active a certain type of soil or mineral is in terms of interacting with its surroundings. In the context of this work, CEC was used as an additional measure to investigate the reactivity of the calcite surface. While it was not the primary focus of this work, it could nevertheless provide additional insight.

Various methods are available for determining CEC. An element common to most of them is the initial saturation of a soil sample with an index cation, the purpose of which is to bind to all available surface sites. The assumption is that the overwhelming quantity of the index cation will dislodge all other cations originally retained by the soil and release them into the exchange solution. By measuring the total number of cations liberated by this process, or by comparing the initial and final amounts of the index cation in solution, CEC can be determined. The exact method to reach this point can vary significantly, however: there are numerous different index cations to choose from, which can be used in different amounts, at different concentrations, and in different conditions. The choice ultimately depends on the type of sample being analyzed, with calcite being one of the more problematic kinds [45].

Calcareous clays and soils prove challenging to many CEC methods because calcite has a tendency to dissolve during the process, artificially inflating the amount of Ca^{2+} in solution [31, 45, 47]. Dissolved cations cannot be distinguished from exchanged cations, which skews results if an unsuitable method is chosen. For instance, the $BaCl_2$ method can dissolve calcite to the point that the measured free cations exceed the number of negative surface sites, overestimating the CEC [31]. On the other hand, in the NH_4Ac method Ca^{2+} from dissolved calcite ends up competing for surface sites with the index cation NH^{4+}, leading to a systematic underestimation of the CEC which is calculated from the difference between the initial and final NH^{4+} concentration [48].

One way to reduce this error is to use an index cation with a much stronger affinity for the soil than Ca^{2+}, which is possible with metal complex solutions. Almost all surface sites should then be

occupied by the index cation, eliminating the issues faced in the NH_4Ac method. However, some systematic errors due to the influence of calcite were still noted to occur when using metal complexes [31]. As such, additional measures to reduce the error are required, the most straightforward of which is minimizing the dissolution of calcite. If the exchange solution is saturated with calcite prior to the experiment, calcite in the sample should no longer be able to dissolve while exchangeable Ca^{2+} should desorb normally [31, 47]. In theory, the CEC value should then be much more accurate with much less error arising from non-exchangeable cations.

In this work, a calcite-saturated cobalt hexamine trichloride, $[Co(NH_3)_6]Cl_3$ solution was used to determine the CEC of calcite samples [31, 33]. MP-AES was used to measure exchangeable cations. A method utilizing silver thiourea had also previously been shown to produce reliable results with calcite, but the process involves numerous steps and requires that a fresh exchange solution be prepared each time [47]. On the other hand, cobalt hexamine trichloride is a well-known reagent that is easy to prepare and does not impose a time limit, while the CEC method itself can be as simple as shaking and filtering the suspension [49]. For this reason, the cobalt hexamine ion was chosen as the index cation, with calcite saturation intended to further improve the results.

3. Experimental work

3.1 Preparation of calcite

Two types of calcite were used in this work: commercial pure calcite purchased from the UK, and calcite samples from the Bukov Underground Research Facility in the Czech Republic [30]. Solid samples of pure and Bukov calcite were sawed off from the rest of the rock material they had been embedded in. The resulting chunks were crushed into smaller pieces and milled into fine grains using a steel ball mill. The grains were sifted through a 25 µm sieve using a brush, with additional milling being done for any particles that were still too large. The resulting fine calcite powder was collected and stored in plastic bags for experimentation.

While specific surface area was not a focus of this work, a small grain size was required to conduct zeta potential measurements as the maximum recommended particle diameter for the Zetasizer device was 10 µm [34]. To ensure the suitability of samples for analysis, calcite particle size was determined using a Microtrac SYNC analyzer and shown to fall within acceptable range. The results are presented in Figures 10 and 11.

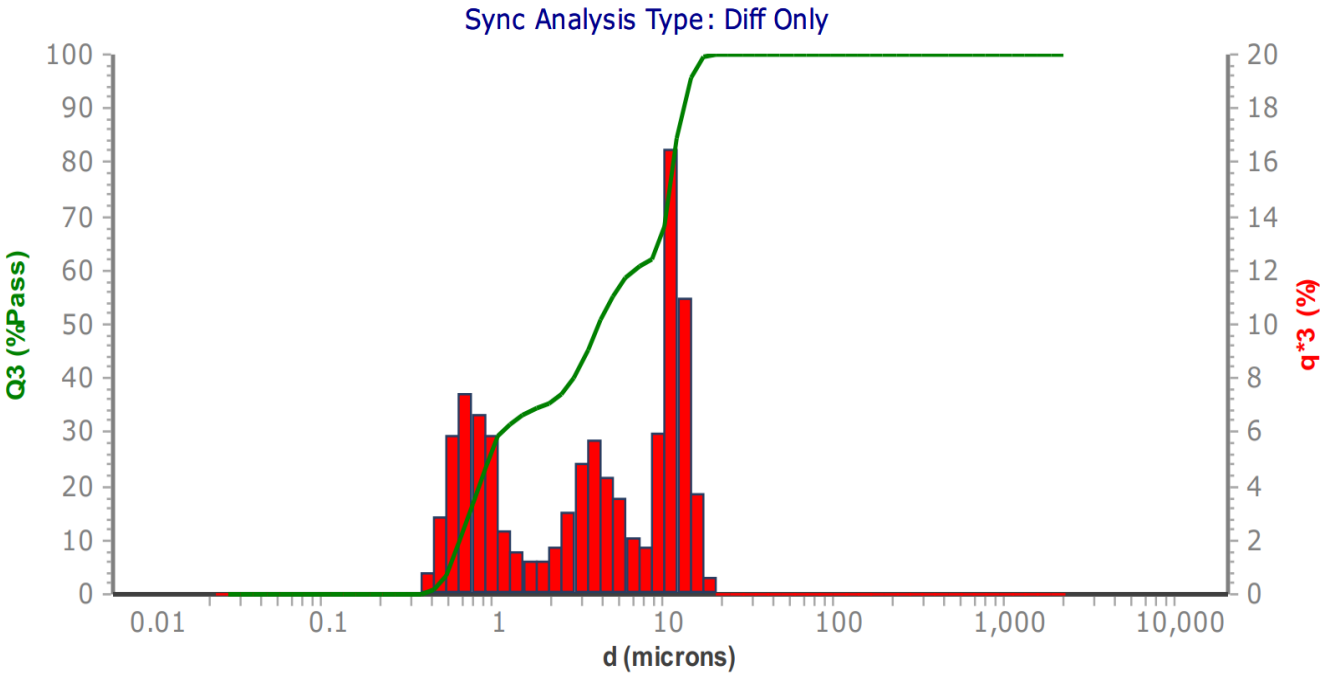

Figure 10. Microtrac SYNC particle size distribution results for pure calcite.

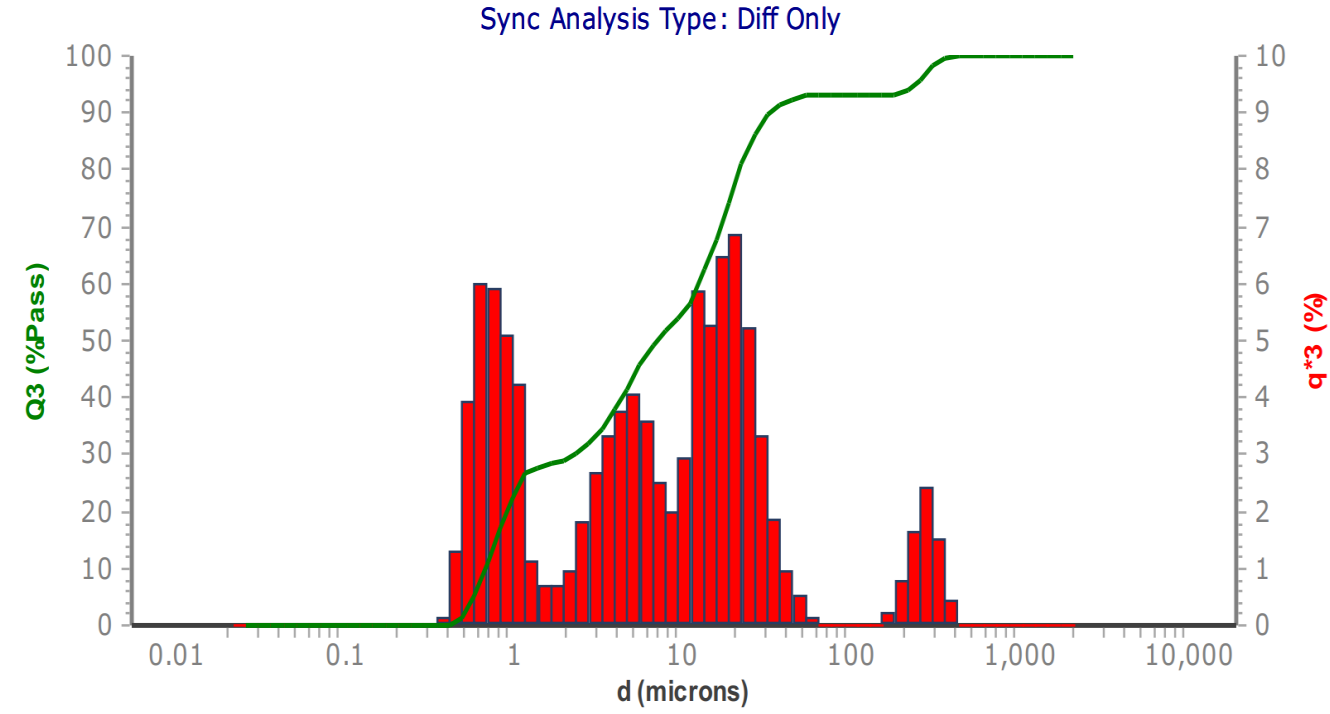

Figure 11. Microtrac SYNC particle size distribution results for Bukov calcite.

3.2 Chemicals and solutions

Several solutions with different ionic compositions and strengths, as well as a SGW2 groundwater simulant, were used in this work to study the behavior of calcite and their effect on surface charge. The chemicals used to prepare the solutions are listed in Table 1, with the solutions themselves contained in Table 2.

Table 1. List of chemicals used in this work.

Chemical	**Manufacturer**	**Molar mass**
$CaCl_2$	Fisher Scientific UK	110.99 g mol^{-1}
NaCl	Fisher Scientific UK	58.44 g mol^{-1}
$MgCl_2 \bullet 6\ H_2O$	Merck	203.30 g mol^{-1}
$MgSO_4 \bullet 7\ H_2O$	Merck	246.48 g mol^{-1}
MgO	Merck	40.31 g mol^{-1}
$Ca(OH)_2$	Merck	74.09 g mol^{-1}
$KHCO_3$	Merck	100.12 g mol^{-1}
$NaHCO_3$	Fisher Scientific UK	84.01 g mol^{-1}
$[Co(NH_3)_6]Cl_3$	Sigma-Aldrich	267.48 g mol^{-1}

Table 2. List of solutions used in this work.

Solution	**Concentration**
$CaCl_2$	0.001 M
NaCl	0.01 M
$MgCl_2$ + NaCl	0.0025 M ($MgCl_2$) + 0.005 M (NaCl)
$MgCl_2$ + NaCl	0.00375 M ($MgCl_2$) + 0.0025 M (NaCl)
$[Co(NH_3)_6]Cl_3$	0.0166 M
SGW2	Contents listed in Table 3

Table 3. Composition of SGW2 (preparation for 5 L).

Chemical	**Amount added (g)**	**Concentration (mol dm^{-3})**
$MgSO_4 \bullet 7\ H_2O$	0.2808	2.28×10^{-4}
MgO	0.0139	6.9×10^{-5}
$MgCl_2 \bullet 6\ H_2O$	0.0501	4.93×10^{-5}
$Ca(OH)_2$	0.3464	9.35×10^{-4}
$KHCO_3$	0.0275	5.49×10^{-5}
$NaHCO_3$	0.3026	7.2×10^{-4}

Abundances of relevant cations and anions in freshly prepared equilibration solutions are presented in Figure 12 for comparison.

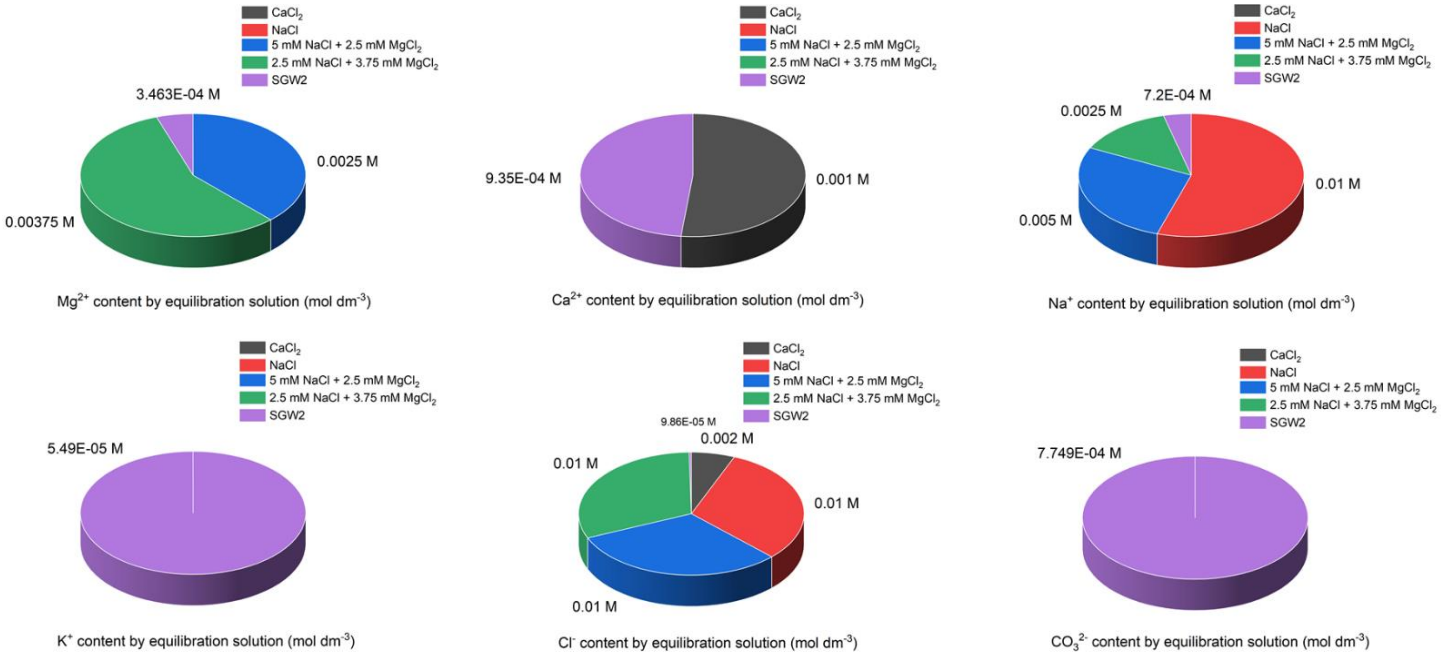

Figure 12. Starting ionic composition of electrolyte solutions used in equilibration.

3.3 General setup for equilibration

Each sample in this work consisted of 0.75 g of prepared calcite weighed into 50 ml centrifuge tubes, which were filled with 50 ml of an equilibration solution. Samples were then be placed in batches of 7 into an unpressurized glove box where they were equilibrated using a CO_2/N_2 gas mixture (250 ppm CO_2). This gas was bubbled directly into each individual sample tube to facilitate the interaction of CO_2 with the solution and reduce the time required for each experiment. No dedicated gas delivery system was available, and a simple custom one was created using a series of flexible plastic tubing that would decrease in diameter in a series of steps. A 5x8 mm tube was connected to the gas bottle, from where it would extend inside the glove box towards a Y-shaped splitter connected to two 3x5 mm tubes on the other end. These tubes would in turn connect to smaller Y splitters with two 2x4 mm tubes on each end leading to T-shaped junctions. These junctions would transfer the gas into 1,3 mm tubes that extended into the sample solution and delivered the gas to the samples. A schematic of this setup is illustrated in Figure 13, with Figures 14 – 16 showing it in practice.

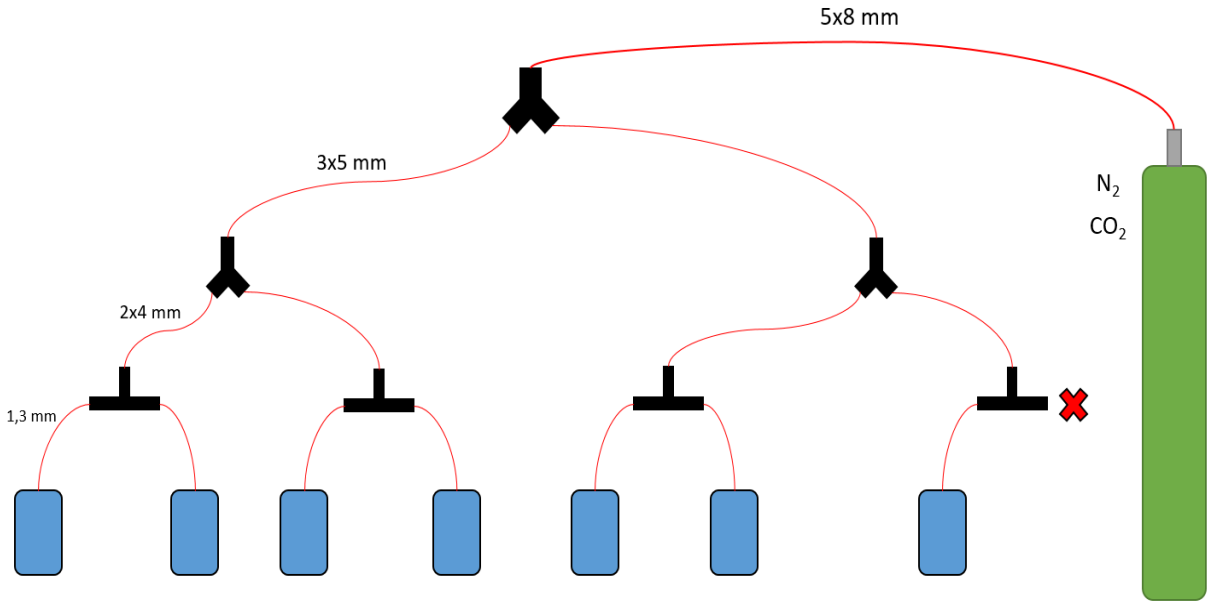

Figure 13. Sketch of the equilibration setup used in this work.

Figure 14. The glove box used in this work.

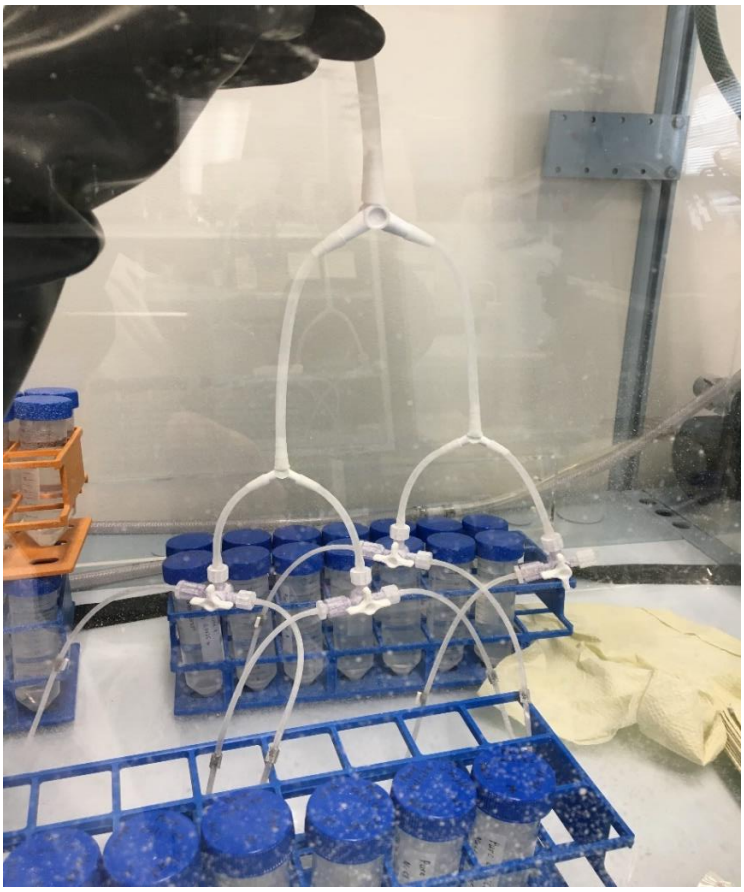

Figure 15. The tubing system as it appeared in practice.

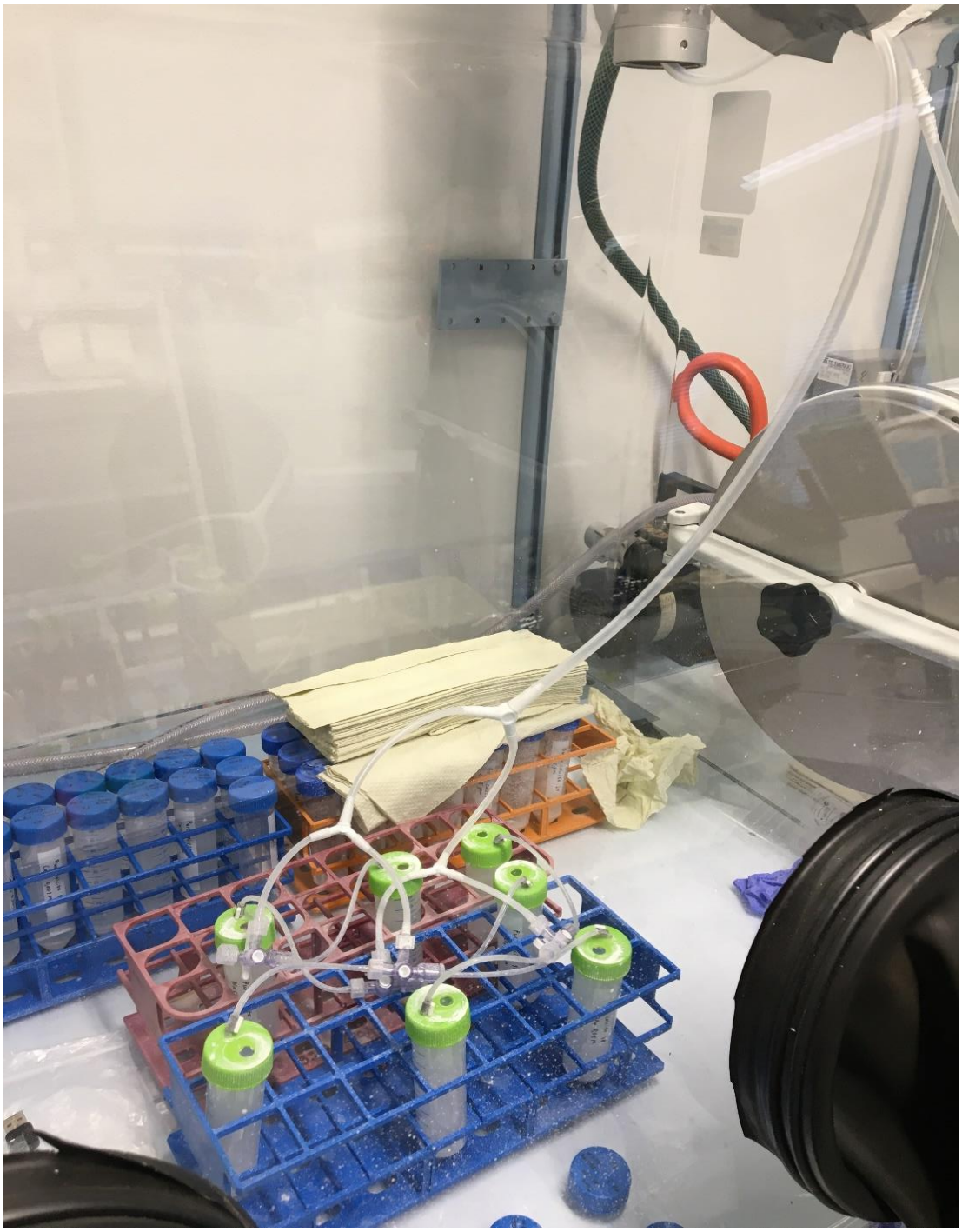

Figure 16. Samples in the process of bubbling.

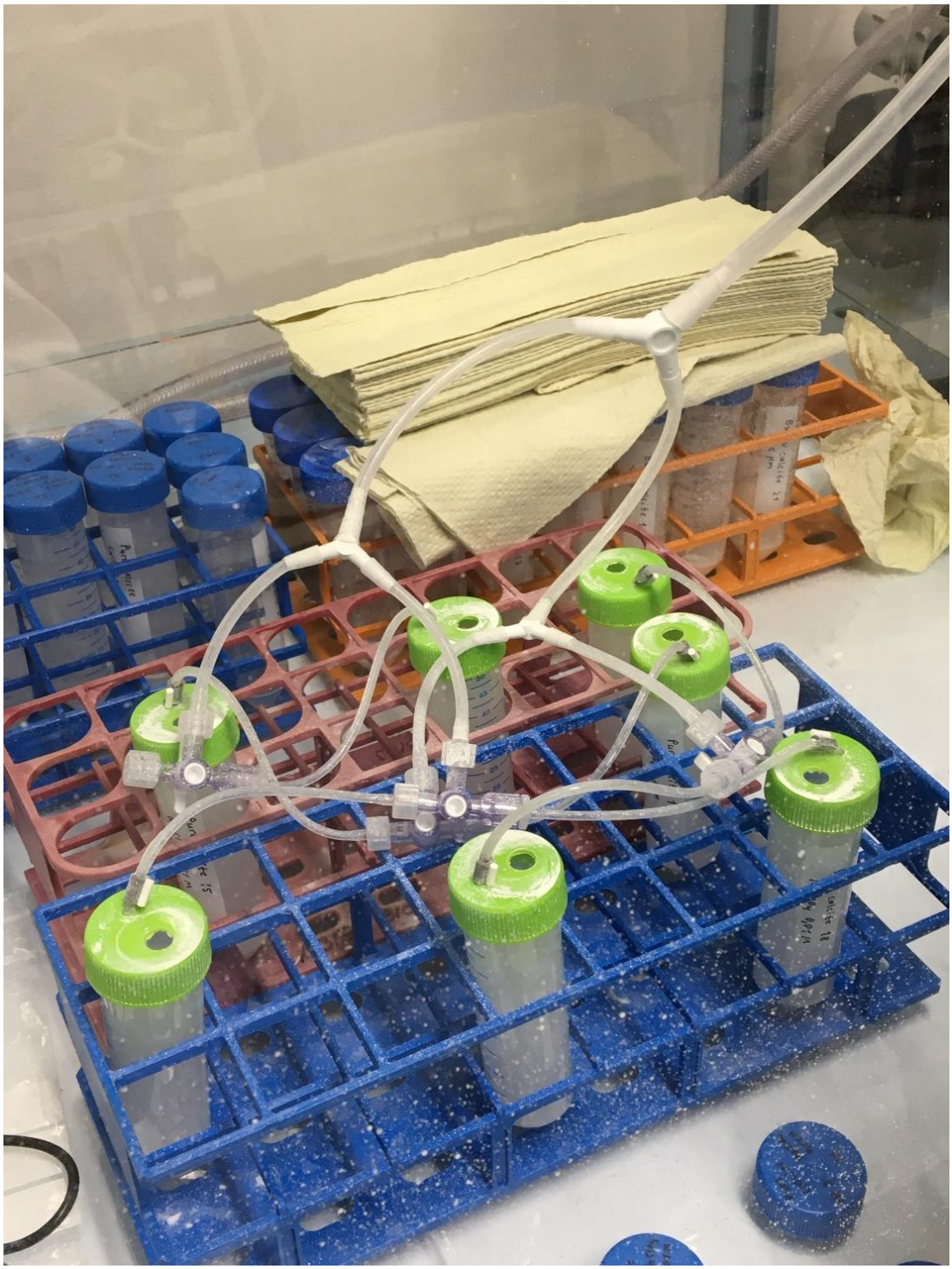

Figure 17. Samples in the process of bubbling (closer view).

In general, each sample batch containing a different combination of calcite and solution would undergo 1-hour long sessions of bubbling either daily or on pre-determined days. On the final day of any given experiment, samples for zeta potential measurements would be taken and measurements performed. Ca concentration was monitored as an indicator of equilibrium and stability of the system using MP-AES, and for this purpose 0.5 ml aliquots were taken from each sample before and after bubbling on each day of the experiment. Between bubbling and the taking of aliquots, sample tubes were stored in the glove box and tightly capped to minimize interactions with the outside atmosphere. Given the number of variables and custom nature of the setup, conditions for different batches vary considerably as they were often revised in response to the results obtained over the course of this work. As a result, the work can be separated into three distinct series of samples, which are best explained individually.

3.4 Series 1 equilibration

Details and experiment conditions for the first series are summarized in Table 4.

Table 4. Summary of Series 1 experiments.

Calcite	Solution	# of samples	Experiment length	pH control	pH range	Bubbling
Pure (0.75 g)	SGW2 (50 ml)	7	3 days	no	≈ 8 - 9	1 h daily
Pure (0.75 g)	$CaCl_2$ (50 ml)	7	5 days	no	≈ 8	1 h daily
Pure (0.75 g)	NaCl (50 ml)	7	5 days	no	≈ 7 – 8.5	1 h daily
Bukov (0.75 g)	SGW2 (50 ml)	7	5 days	no	≈ 9.5	1 h daily
Bukov (0.75 g)	$CaCl_2$ (50 ml)	7	5 days	no	≈ 8 – 8.5	1 h daily
Bukov (0.75 g)	NaCl (50 ml)	7	5 days	no	≈ 8 – 8.5	1 h daily
Bukov (0.75 g)	NaCl (50 ml)	7	3 days (continued)	yes	7.8 - 9	1 h daily

For the first series of samples, emphasis was placed on validating the equilibration procedure. Samples were bubbled for 1 h daily using the CO_2/N_2 mixture, with 0.5 ml aliquots being taken each day before and after bubbling. 3 days were estimated to be sufficient to establish equilibrium, but for samples following the pure calcite/SGW2 batch the length was increased to 5 days to produce more reliable results, dedicating a week of daily 1-h bubbling to each. pH was not controlled at this stage and merely measured and recorded to observe trends. Zeta potentials were also not yet measured with the exception of the final Bukov calcite/NaCl batch, which was continued directly from the previous week. This batch served as a test run for future experiments and was the only one in the series where pH control was attempted in the range of 7.8 – 9 by adding HCl/NaOH each day prior to bubbling.

For MP-AES measurements, all 0.5 ml sample aliquots were diluted to 10 ml using the appropriate equilibration solution, and 360 µl concentrated HNO_3 as well as 100 µl of a Cs buffer solution were added to each. A series of 10 ml standard solutions was prepared for each equilibration solution. Each standard contained the following cations: Mg, Al, Mn, Na, K, Fe and Ca. Standard concentrations were 0 ppm, 0.5 ppm, 1 ppm, 5 ppm, 20 ppm and 50 ppm. Standard solutions were made using their respective equilibration solutions, with the rest of the volume being made up through individual elemental standard additions. Standards also received 360 µl of concentrated HNO_3 and 100 µl of Cs buffer each.

For zeta potential measurements, approximately 0.9 ml were drawn directly from each sample after centrifugation (10 min, 4500 rpm) and transferred to Zetasizer cells.

3.5 Series 2 equilibration

Details and experiment conditions for the second series are summarized in Table 5.

Table 5. Summary of Series 2 experiments.

Calcite	Solution	# of samples	Experiment length	pH control	pH range	Bubbling
Pure (0.75 g)	SGW2 (50 ml)	7	5 days	yes	6.5 – 11	1 h / 3 days
Pure (0.75 g)	NaCl (50 ml)	7	5 days	yes	6.5 – 11	1 h / 3 days
Pure (0.75 g)	$MgCl_2$ + NaCl 2.5 mM + 5 mM (50 ml)	7	5 days	yes	6.5 – 11	1 h / 3 days
Pure (0.75 g)	$MgCl_2$ + NaCl 3.75 mM + 2.5 mM (50 ml)	7	5 days	yes	6.5 – 11	1 h / 3 days

In the second series, zeta potential measurements began in earnest. Samples were bubbled for 1 h at a time using the same CO_2/N_2 mixture, and 0.5 ml aliquots were taken before and after. However, bubbling was now performed only during the first 3 days, allowing the samples to sit and stabilize undisturbed for the remaining 2 days. pH was also regularly controlled with the addition of HCl/NaOH, and the pH range was expanded to 6.5 – 11. Each sample had its own pH value that increased between samples in the following increments: 6.5 – 7.5 – 8.5 – 9 – 9.5 – 10.5 – 11. In addition, pH adjustments were now made after bubbling as the process was noted to significantly disturb the solution's pH, rendering any adjustments made beforehand pointless. For the last 2 days where no bubbling occurred, only the pH was monitored and adjusted if necessary, with aliquots being taken before and after measurement/adjustment. On the final day, after the final pH adjustment, 3 hours were allowed to pass to let the solution stabilize before samples for zeta potential measurements were taken.

For MP-AES measurements, all 0.5 ml sample aliquots were diluted to 5 ml using deionized water, and 180 µl of concentrated HNO_3 as well as 50 µl of a Cs buffer solution were added to each. A series

of 10 ml standard solutions was prepared for each equilibration solution. Each standard contained the following cations: Mg, Al, Mn, Na, K, Fe and Ca. Standard concentrations were 0 ppm, 0.5 ppm, 1 ppm, 5 ppm, 10 ppm, 20 ppm and 50 ppm. Standard solutions were made in the same dilution ratio as the aliquots (1/10) using deionized water and their respective equilibration solutions. Standards also received 360 µl of concentrated HNO_3 and 100 µl of Cs buffer each. In addition, 50 ml solutions containing 2 ppm of Ca were prepared from each equilibration solution to act as external standards. These solutions followed the same 1/10 solution/water ratio and received 1.8 ml of concentrated HNO_3 as well as 500 µl of Cs buffer.

For zeta potential measurements, approximately 0.9 ml of solution were drawn directly from each sample after centrifugation (10 min, 4500 rpm) and transferred to Zetasizer cells.

3.6 Series 3 equilibration

Details and experiment conditions for the third series are summarized in Table 6.

Table 6. Summary of Series 3 experiments.

Calcite	Solution	# of samples	Experiment length	pH control	pH range	Bubbling
Pure (0.75 g)	SGW2 (50 ml)	7	1 month	yes	6.5 – 11	1 h / 2x per week
Pure (0.75 g)	NaCl (50 ml)	7	1 month	yes	6.5 – 11	1 h / 2x per week

In the third series, the equilibrium achieved using the bubbling method was investigated on a longer timescale. NaCl and SGW2 batches from the second series were selected to undergo further studies to determine if equilibrium had actually been reached or if the samples had not yet fully stabilized in the previous experiments. These batches were bubbled twice every week for 1 h at a time over the course of 1 month, with 0.5 ml aliquots taken before and after each bubbling session. pH control was performed using HCl/NaOH to keep samples in the range of pH 6.5 – 11. The same pH increments as in Series 2 were used, and adjustments were still made after bubbling. On the final week, no bubbling was done on the last 2 consecutive days of the experiment, and samples for zeta potential measurements were taken on the final day after a 3-hour wait following pH adjustment.

For MP-AES measurements, all 0.5 ml sample aliquots were diluted to 5 ml using deionized water, and 180 µl of concentrated HNO_3 as well as 50 µl of a Cs buffer solution were added to each. The same standard solutions from Series 2 were used (10 ml, 0-50 ppm, Mg + Al + Mn + Na + K + Fe + Ca). In addition, fresh 50 ml solutions containing 2 ppm of Ca were prepared from both equilibration solutions to act as external standards, following the same solution/water ratio and receiving 1.8 ml of concentrated HNO_3 as well as 500 µl of Cs buffer.

For zeta potential measurements, approximately 0.9 ml of solution were drawn directly from each sample after centrifugation (10 min, 4500 rpm) and transferred to Zetasizer cells.

3.7 Cation exchange capacity

Two separate 0.0166 M exchange solutions of $[Co(NH_3)_6]Cl_3$ were prepared for Bukov and pure calcite samples. 0.25 g of prepared Bukov calcite were added to one solution and 0.25 g of prepared pure calcite were added to the other. The suspensions were placed in an ultrasonic bath for 30 min, after which both were magnetically stirred for another 30 min. The suspensions were then left to equilibrate until the experiment could be performed. In this case equilibration lasted approximately two weeks, but leaving the solutions overnight should otherwise be sufficient [33].

CEC samples consisted of 1 g of fine-grained calcite weighed into 20-ml centrifuge tubes for a total of 6 samples: 3 containing Bukov calcite and 3 containing pure calcite. 10 ml of $[Co(NH_3)_6]Cl_3$ solution saturated with the appropriate type of calcite were added to each sample, after which the samples were shaken for 1 h. 0.5 ml supernatants were taken from each sample to measure Ca, and separate 5 ml supernatants were collected for the determination of other ions.

For MP-AES measurements, the 0.5 ml supernatants were diluted to 5 ml using deionized water, and 180 µl of concentrated HNO_3 as well as 50 µl of a Cs buffer solution were added to each. Two separate series of 10 ml standard solutions were made for Bukov and pure calcite samples respectively. Each standard only contained Ca. Standard concentrations were 0 ppm, 25 ppm, 50 ppm, 75 ppm and 100 ppm. Standard solutions were made in the same dilution ratio as the supernatants (1/10) using deionized water and the exchange solution saturated with the appropriate type of calcite. Standards also received 360 µl of concentrated HNO_3 and 100 µl of Cs buffer each. In addition, two 50 ml solutions containing 2 ppm of Ca were prepared from the exchange solutions to act as external standards, following the same 1/10 solution/water ratio and receiving 1.8 ml of concentrated HNO_3 as well as 500 µl of Cs buffer each. These solutions were

identical with the exception of the type of calcite they were saturated with and were used with their respective sample and standard series. Only Ca was measured with these samples.

The 5 ml supernatants were diluted to 10 ml using deionized water, and 360 µl concentrated HNO_3 as well as 100 µl of a Cs buffer solution were added to each. Two separate series of 10 ml standard solutions were made for Bukov and pure calcite samples respectively. Each standard contained the following cations: Mg, Al, Mn, Na, K and Fe. Standard concentrations were 0 ppm, 0.25 ppm, 0.5 ppm, 0.75 ppm and 1 ppm. 250 µl of 1000 ppm Ca were also added to each standard to ensure a similar background level. Standard solutions were made in the same dilution ratio as the supernatants (1/2) using deionized water and the exchange solution saturated with the appropriate type of calcite. Standards also received 360 µl of concentrated HNO_3 and 100 µl of Cs buffer each. In addition, two 50 ml solutions containing 2 ppm of each previously mentioned cation were prepared from the exchange solutions to act as external standards. These solutions followed the same 1/2 solution/water ratio and received 1.8 ml of concentrated HNO_3, 500 µl of Cs buffer, and 1.25 ml of 1000 ppm Ca each. They were also identical except for their type of calcite saturation.

4. Results

4.1 Uncertainty estimation

Uncertainty values of MP-AES results obtained in this work were estimated using the Measurement Uncertainty kit (MUkit software) [50, 51]. The program combines random and systematic error components to produce a final combined standard uncertainty according to the following equation:

$$u_c = \sqrt{u_{Rw}^2 + u_b^2} \tag{2}$$

where u_{Rw} is the uncertainty component for intralaboratory reproducibility (random error), and u_b is the uncertainty component for method and laboratory bias (systematic error). The result is then used to calculate the expanded uncertainty U in order to reach a high enough confidence interval:

$$U = k \times u_c \tag{3}$$

where k is an integer. In general, k is set to 2, which achieves a confidence interval of about 95%.

4.2 Cation exchange capacity

CEC was calculated with the following equation:

$$CEC = \sum \frac{C \times V \times Z}{m \times M} \quad (4)$$

where C is the concentration of an individual exchangeable cation (ppm = mg/l), V is the volume of the solution (l), Z is the charge of the cation, m is the mass of calcite used in the experiment (mg), and M is the molar mass of the cation (g/mol). V was constant (10 ml = 0.01 l), as well as m (1 g = 1000 mg). The values used for Z and M are listed in Table 7.

Table 7. Exchangeable cation Z and M values.

	Mg	**Al**	**Mn**	**Na**	**K**	**Fe**	**Ca**
Z	2	3	2	1	1	2	2
M (g/mol)	24.305	26.982	54.938	22.99	39.098	55.845	40.078

The MP-AES detection limit was calculated for each relevant element with the following equation using the Currie method [52]:

$$N_D = 4.65 \times \sqrt{N_B} + 2.71 \quad (5)$$

where N_B is the number of counts recorded in a blank sample.

4.2.1 Bukov calcite cation exchange capacity

Below are the MP-AES results obtained from the solution saturated with Bukov calcite. The values are corrected for dilution and device performance based on the external standard. Background subtraction is also performed on the sample average based on blank measurements.

Table 8. Bukov calcite CEC results (MP-AES).

	Mg (ppm)	Al (ppm)	Mn (ppm)	Na (ppm)	K (ppm)	Fe (ppm)	Ca (ppm)
Sample 1	1.70	0.267	<6.54E-03	0.800	0.441	<0.369	25.9
Sample 2	1.56	0.296	<6.54E-03	0.575	0.312	<0.369	21.9
Sample 3	1.70	0.334	0.0293	0.604	0.277	<0.369	23.1
Blank 1	<2.24E-03	0.0630	<6.54E-03	<3.13E-03	<5.00E-03	<0.369	1.07
Blank 2	<2.24E-03	0.0200	<6.54E-03	<3.13E-03	<5.00E-03	<0.369	1.90
Blank 3	<2.24E-03	0.0380	<6.54E-03	<3.13E-03	<5.00E-03	<0.369	1.82
Average	*1.65 ± 0.545*	*0.259 ± 0.0803*	*0.00976 ± 0.0512*	*0.660 ± 0.409*	*0.343 ± 0.233*	*x*	*22.1 ± 8.62*

Detection limits were calculated from average intensity values from blank measurements using Equation 5 and MP-AES calibration data, shown with Al:

$$N_D(cps) = 4.65 \times \sqrt{329.2366667} + 2.71 = 87.08369155$$

Al calibration equation obtained from device:

$$Intensity = 17269.04898417 \times C$$

Detection limit:

$$N_D(ppm) = \left(\frac{87{,}08369155}{17269.04898417}\right) \times 2(dilution\ factor) = 0.010085523\ ppm \approx 0.01\ ppm$$

Insufficient counts were obtained from most other elements to calculate every N_D in this way. As such, for elements other than Al and Ca, N_D was extrapolated by relating the detection limit calculated for Al to its internal intensity value the MP-AES used for calibration in this measurement. By multiplying N_D (Al) by the ratio of intensities, N_D was obtained as follows:

$$N_D(element, ppm) = N_D(Al, ppm) \times \frac{Intensity_{Al}}{Intensity_{element}}$$

CEC was calculated by applying Equation 4 to each individual cation in the following manner, shown with Mg:

$$CEC(Mg) = \frac{1.65 \frac{mg}{l} \times 0.01\ l \times 2}{1000\ mg \times 24.305 \frac{g}{mol}} = 1.35775 \times 10^{-6} \frac{mol}{g}$$

Values calculated for each ion are compiled in Table 9.

Table 9. Bukov calcite individual ion CEC values.

	Mg (mol/g)	**Al (mol/g)**	**Mn (mol/g)**	**Na (mol/g)**	**K (mol/g)**	**Fe (mol/g)**	**Ca (mol/g)**
CEC	1.36E-06	2.88E-07	3.55E-09	2.87E-07	8.77E-08	0	1.10E-05

The sum of all values in Table 9 gives the total CEC for Bukov calcite, presented in Table 10.

Table 10. Bukov calcite CEC results.

CEC	**mol/g**	**mmol/g**	**meq/100 g**	**meq/kg**
Bukov calcite	1.31E-05	0.0131	1.31	13.1

4.2.2 Pure calcite cation exchange capacity

Below are the MP-AES results obtained from the solution saturated with pure calcite. The values are corrected for dilution and device performance based on the external standard. Background subtraction is also performed on the final sample average based on blank measurements.

Table 11. Pure calcite CEC results (MP-AES).

	Mg (ppm)	**Al (ppm)**	**Mn (ppm)**	**Na (ppm)**	**K (ppm)**	**Fe (ppm)**	**Ca (ppm)**
Sample 1	0.469	0.0730	<7.18E-03	0.167	0.0444	<0.536	8.36
Sample 2	0.446	0.104	<7.18E-03	0.140	0.0626	<0.536	10.3
Sample 3	0.386	0.0994	<7.18E-03	0.117	0.0202	<0.536	9.96
Blank 1	<2.88E-03	0.0447	<7.18E-03	<3.32E-03	<6.17E-03	<0.536	2.07
Blank 2	<2.88E-03	0.0211	<7.18E-03	<3.32E-03	<6.17E-03	<0.536	2.05
Blank 3	<2.88E-03	0.0437	<7.18E-03	<3.32E-03	<6.17E-03	<0.536	2.22
Average	*0.434 ± 0.152*	*0.0556 ± 0.0267*	*x*	*0.141 ± 0,0776*	*0.0424 ± 0.0441*	*x*	*7.43 ± 2,45*

N_D and CEC were calculated in the same way as for Bukov calcite. CEC values calculated for each ion are compiled in Table 12.

Table 12. Pure calcite individual ion CEC values.

	Mg (mol/g)	**Al (mol/g)**	**Mn (mol/g)**	**Na (mol/g)**	**K (mol/g)**	**Fe (mol/g)**	**Ca (mol/g)**
CEC	3.57E-07	6.18E-08	0	6.13E-08	1.08E-08	0	3.71E-06

The sum of all values in Table 12 gives the total CEC for pure calcite, presented in Table 13.

Table 13. Pure calcite CEC results.

CEC	**mol/g**	**mmol/g**	**meq/100 g**	**meq/kg**
Pure calcite	4.20E-06	0.00420	0.420	4.20

4.2.3 Cation exchange capacity summary

CEC results from both types of calcite are presented in Table 14 for comparison.

Table 14. CEC results summary.

CEC	**mol/g**	**mmol/g**	**meq/100 g**	**meq/kg**
Bukov calcite	1.31E-05	0.0131	1.31	13.1
Pure calcite	4.20E-06	0.00420	0.420	4.20

Bukov calcite shows a much higher CEC value than pure calcite. As CEC is a method to quantify negatively charged surface sites, this would suggest that Bukov calcite contains a larger number of such sites, and thus its capacity to retain cations is greater. This can likely be attributed to its composition: compared to pure calcite, Bukov calcite may contain certain impurities with properties that differ from calcite. These impurities could each have a capacity for cation exchange that is also different from calcite, which in turn would affect the final CEC value for the whole sample. Given the difference in magnitude between the CEC of pure and Bukov calcite samples, the effect caused by such impurities also seems to be rather significant.

These results may be a useful foundation for interpreting the results of equilibration and zeta potential of calcite. Impurities in the calcite mineral could lead to a variable surface structure with regions that interact with the environment differently from a surface that consists entirely of calcite. As such, surface chemistry in Bukov calcite could be more complicated and less predictable, heavily depending on the kind of impurities present. The high CEC value relative to pure calcite could thus indicate that because of its impurities, Bukov calcite might interact with its surrounding solution more actively overall, adsorbing and releasing cations at a higher rate. High ion throughput would be detrimental to zeta potential measurements as it would mean that the calcite surface charge is constantly changing as different ions are cycled in and out. As such, due to a larger number of charged surface sites, surface reactions in Bukov calcite may naturally take longer to reach

equilibrium and could be more prone to disturbances than pure calcite. Surface chemistry could still be an actively ongoing process at the time of the zeta potential measurement, which might lead to poor results.

Bukov calcite's high CEC may also affect the equilibration of potential-determining ions in solution. If the Bukov samples were able to retain and release more cations than pure calcite, higher fluctuations in Ca concentration could be expected. Different cations could be adsorbed and released in different quantities at different times, including Ca^{2+}. Thus, ongoing cation exchange could potentially lead to increases and decreases in the concentration of Ca at different points in time in addition to the effects caused by calcite dissolution and precipitation. At its core, this phenomenon is no different from the mechanisms that would occur in pure calcite, where adsorption and release of Ca^{2+} would also affect the Ca concentration in solution. However, this may only be a noticeable issue in Bukov calcite due to its greater CEC. In these circumstances, Ca concentration in the solution could be inherently more unstable due to Bukov calcite taking up and releasing non-negligible quantities of the cation. This effect may be further compounded if, for instance, conditions in the sample are regularly disturbed by the bubbling of CO_2 into the solution, which was a key part of this work. Ultimately, there does not seem to be any reason why Bukov calcite would fail to equilibrate: the reactions and mechanisms are largely the same as in pure calcite and may simply require more time due to occurring on a larger scale and accounting for impurities.

Lastly, the CEC values obtained in this work may be a reflection of the smaller particle size of calcite. The same CEC experiment was performed in an earlier work with grain sizes between 71 µm and 300 µm, resulting in values of 5.868 meq/kg for Bukov calcite (≈ 45% of this work) and 1.377 meq/kg for pure calcite (≈ 33% of this work) [33]. While Bukov calcite was also found to have a much higher CEC than pure calcite just like in this work, the CEC values themselves were much smaller. This difference can likely be attributed to particle size: the size range in the earlier work was much greater and the smallest grain size was at least 7 times larger than the average size achieved in this work (Figures 10-11). As such, the larger surface area of small particles likely increased the interactions between the calcite and its surrounding solution in this work, leading to a more active exchange of cations and thus much larger CEC values.

4.3 Series 1 equilibration

4.3.1 S1 Pure calcite equilibration

Below are the MP-AES results for pure calcite samples from the initial equilibration experiments.

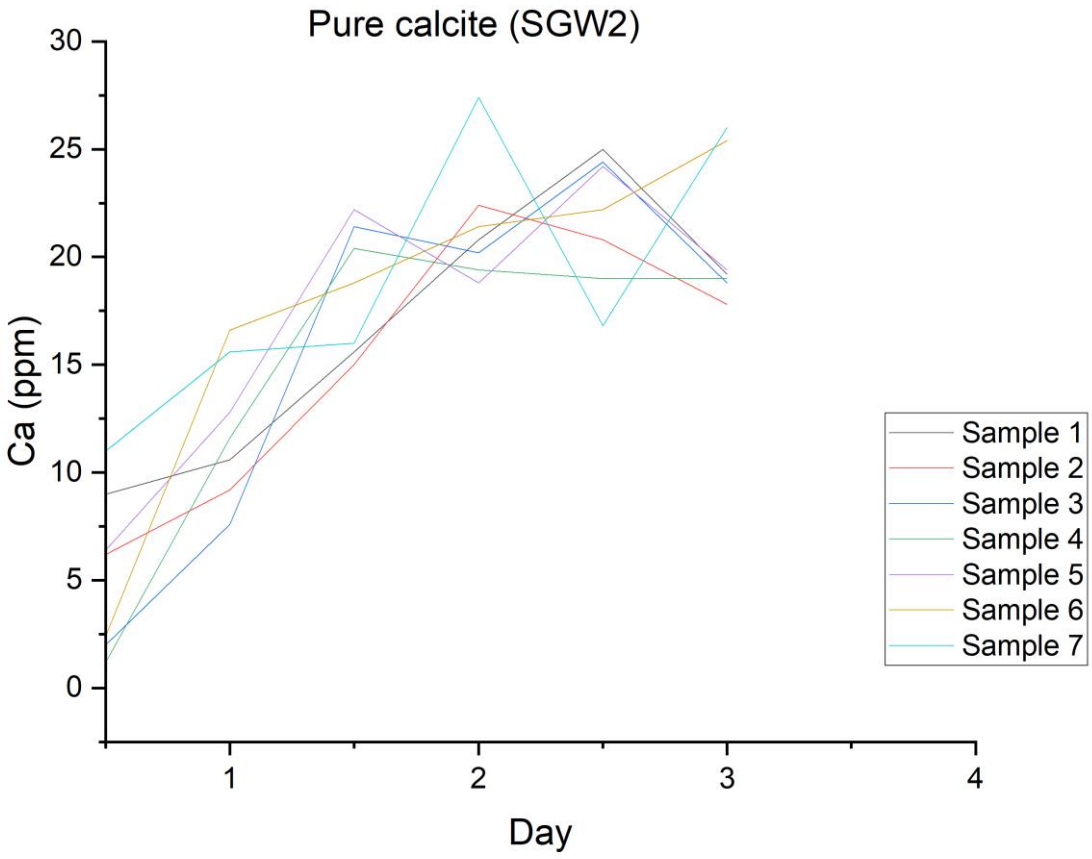

Figure 18. Series 1 Pure calcite/SGW2 equilibration results.

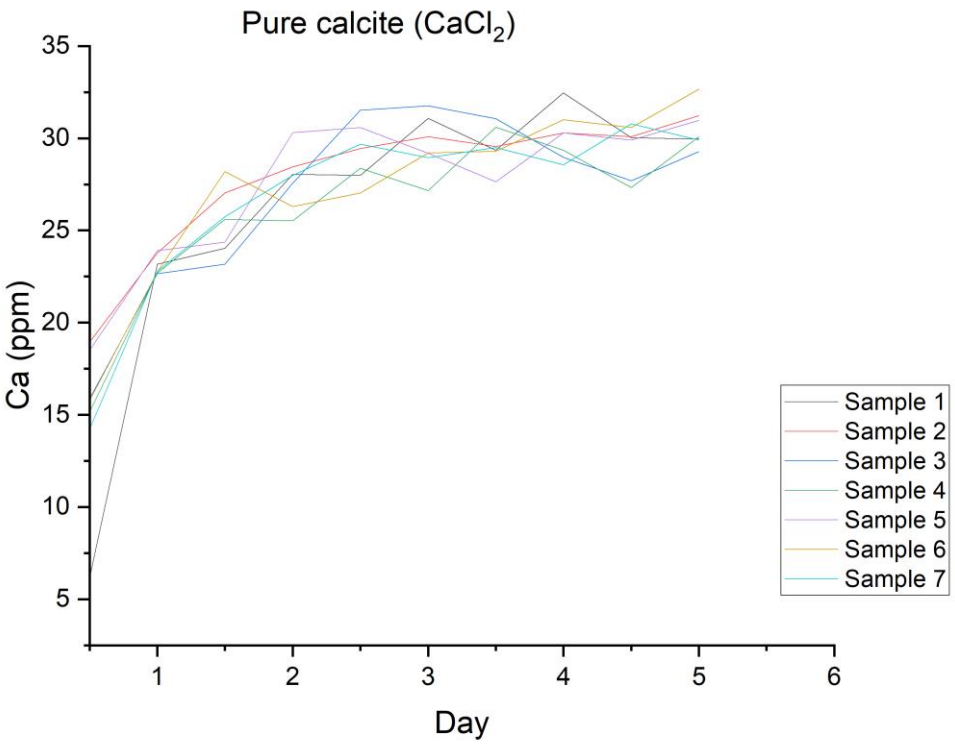

Figure 19. Series 1 Pure calcite/$CaCl_2$ equilibration results.

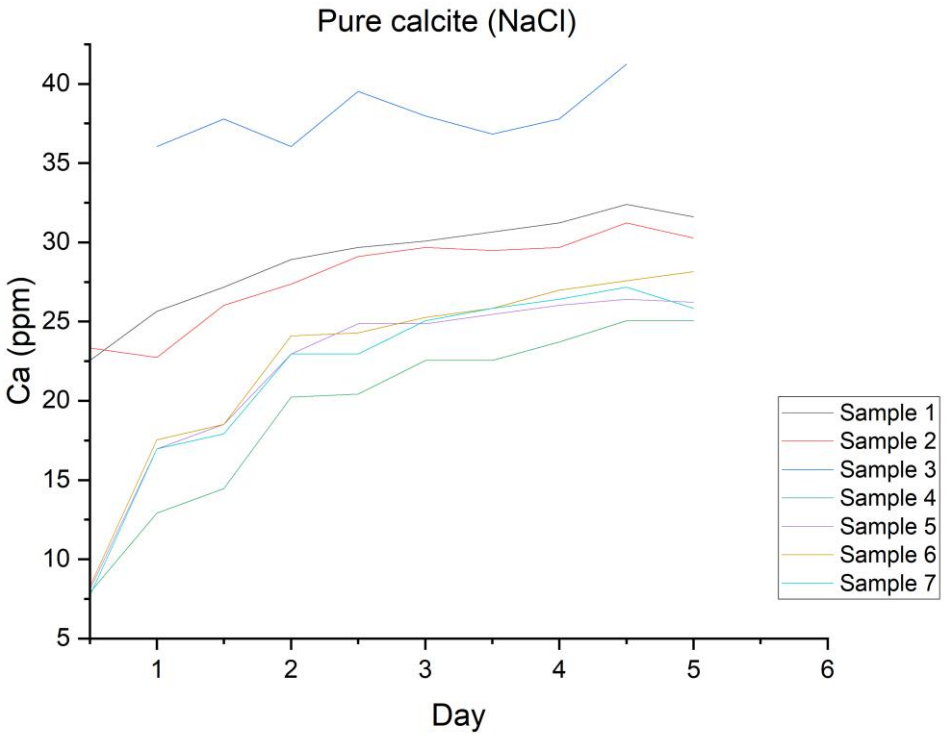

Figure 20. Series 1 Pure calcite/NaCl equilibration results.

Pure calcite samples seem to show an overall trend towards stability. In general, the bubbling of CO_2 initially coincides with a noticeable increase in dissolved Ca content, after which Ca concentration stays relatively stable with minor fluctuations around a certain value. The biggest change tends to occur after the first bubbling session, with subsequent sessions also affecting the Ca concentration but to a much lesser extent. Over time, most samples appear to gradually plateau around a certain concentration, with increases and decreases becoming steadily smaller in magnitude.

While true stability was never achieved, it seems possible to lower the fluctuation of Ca concentration to the point where it may no longer be significant. An important factor to consider is time: as can be seen in Figure 18, the beginning of a plateau is observed, but considerable fluctuation still occurs and it cannot be predicted how the sample would continue to behave. On the other hand, Figures 19 and 20 were produced from experiments that lasted two days longer than the one in Figure 18, and the trend is much clearer. The curves begin to resemble straight lines more as time passes, becoming tightly packed near a particular Ca concentration in Figure 18 or stabilizing around different values in Figure 20. Some fluctuation is always observed in all samples, with the amount of Ca generally increasing after each bubbling session and decreasing overnight. However, the overall trend appears to be a trajectory towards a concentration from which the sample does not deviate significantly. Beyond that point, increases and decreases seem to be temporary and mainly caused by disturbances to the samples by repeated bubbling and exposure to air for the taking of aliquots. Lastly, the samples did not behave identically, with some requiring more time to reach a stable concentration than others. These differences can likely be eliminated simply by extending the duration of any given experiment, however.

Overall, pure calcite appears to equilibrate well using the bubbling method in all solutions that were tested (SGW2, $CaCl_2$, NaCl).

4.3.2 S1 Bukov calcite equilibration

Below are the MP-AES results for Bukov calcite samples from the initial equilibration experiments, as well as the first zeta potentials for the final batch.

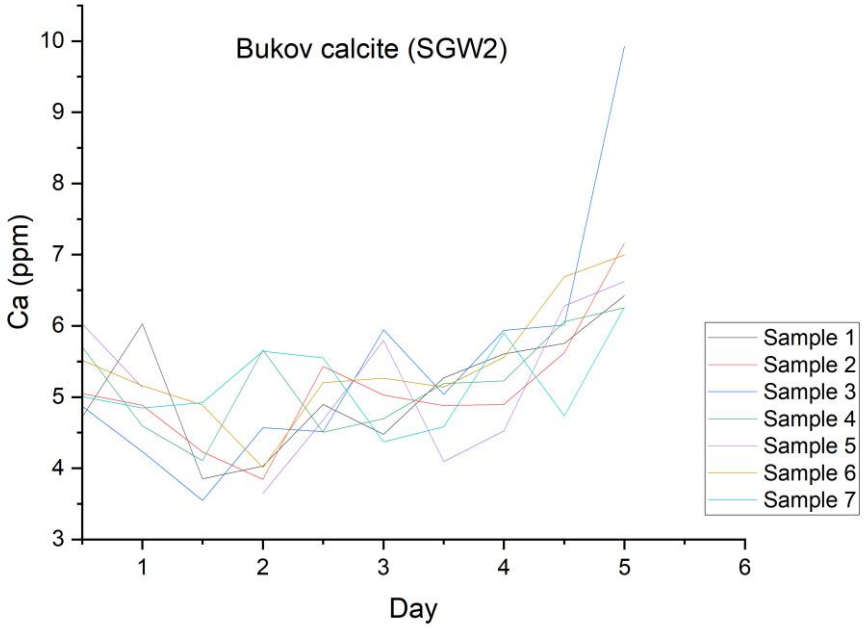

Figure 21. Series 1 Bukov calcite/SGW2 equilibration results.

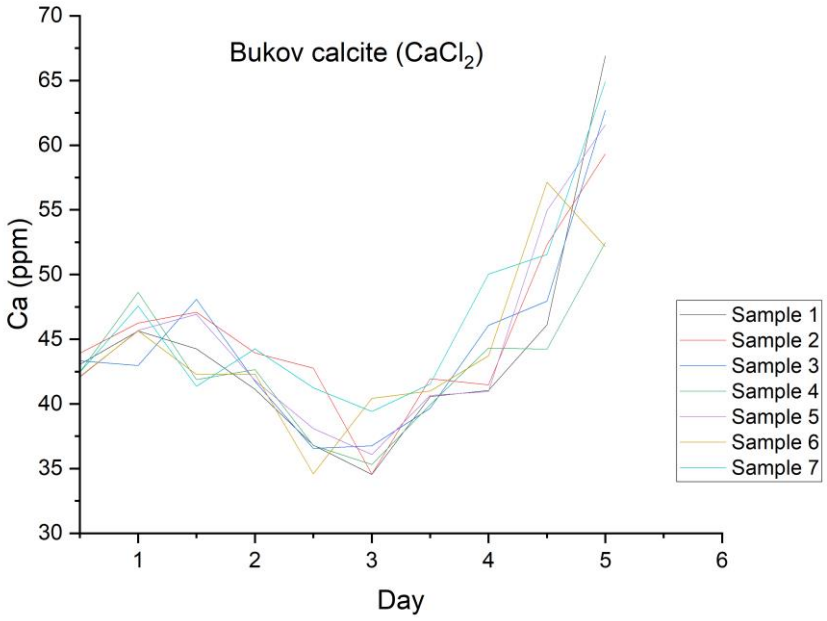

Figure 22. Series 1 Bukov calcite/$CaCl_2$ equilibration results.

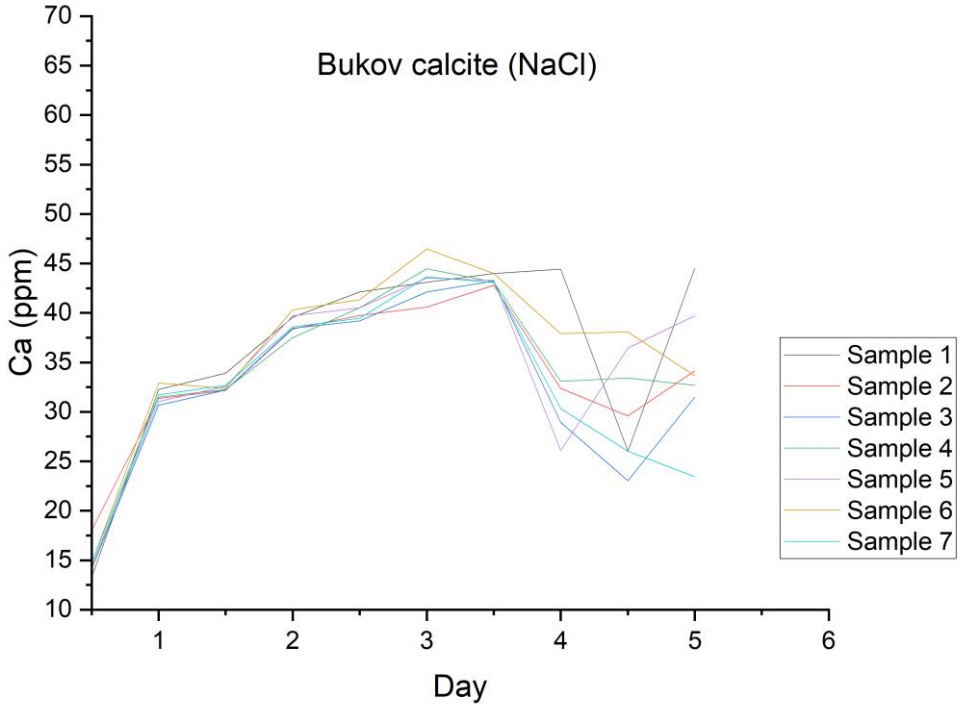

Figure 23. Series 1 Bukov calcite/NaCl equilibration results.

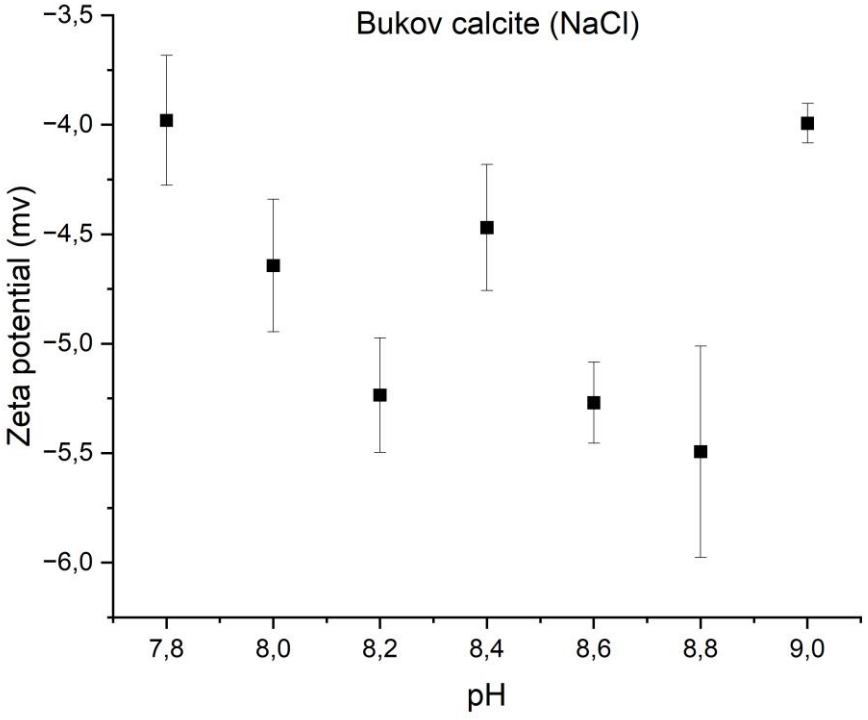

Figure 24. Series 1 Bukov calcite/NaCl zeta potential results.

Bukov calcite samples seem significantly less stable and predictable than pure calcite. No real trend can be observed in any of the graphs: Ca concentration only rises after the initial bubbling in the case of NaCl (Figure 23), where the shape of the curves starts to resemble the results obtained from pure calcite, but after the third day all samples seem to break apart into random concentrations. In Figures 21 and 22, the initial increase in Ca concentration is either minor or non-existent, with Figure 21 even showing a decrease in Ca concentration after the first bubbling session. Ca appears to fluctuate randomly over a wide range of concentrations, and the samples never properly converge or stabilize.

The lack of stability is further illustrated by zeta potentials in Figure 24, which were measured from the NaCl solution containing Bukov calcite. The sample batch in question was first equilibrated for 5 days like the rest, and then underwent an additional 3 days of equilibration combined with pH control over a fairly narrow range (7.8 – 9). However, even with the differences between sample pH values being relatively small, the zeta potentials of different samples are still far too close in value to one another with ± 1.5 mV of difference at most, while also appearing randomly distributed with large margins of error. Results such as these might suggest that the system was not in equilibrium, with ongoing surface chemistry constantly altering the zeta potential.

Overall, equilibration of Bukov calcite using the bubbling method appears to be less effective than pure calcite. As could be inferred from CEC results, the magnitude of the fluctuations in Ca concentration and the unpredictable shapes of the curves suggest that the issue does not lie with simple adjustable variables like time, but rather originates from the inherent properties of Bukov calcite. As such, the equilibration method used in this work was deemed unsuitable for it, and the use of Bukov calcite in all subsequent experiments was discontinued.

4.4 Series 2 equilibration

Below are the MP-AES and zeta potential results from the second sample batch (only pure calcite).

4.4.1 S2 Pure calcite in synthetic groundwater (SGW2)

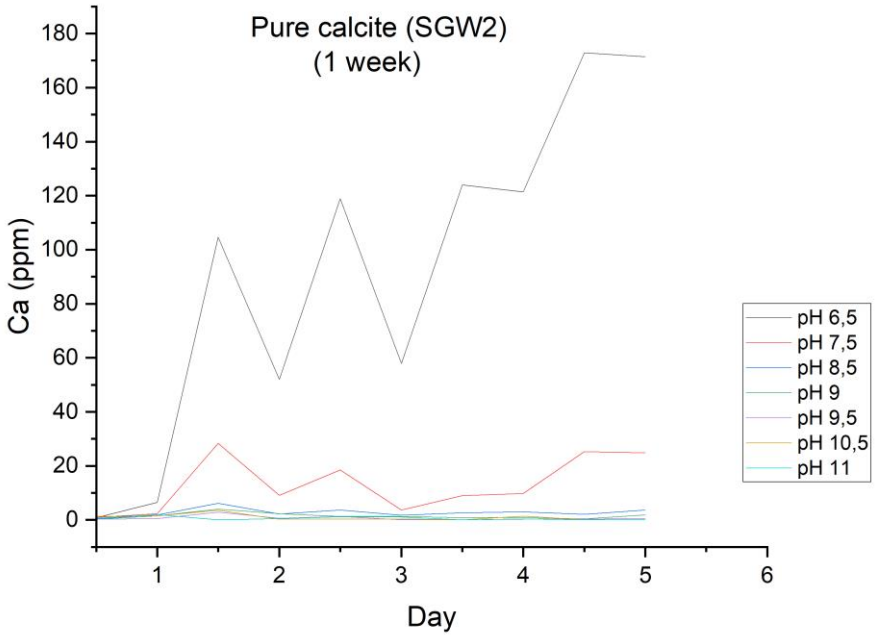

Figure 25. Series 2 Pure calcite/SGW2 equilibration results (full scale).

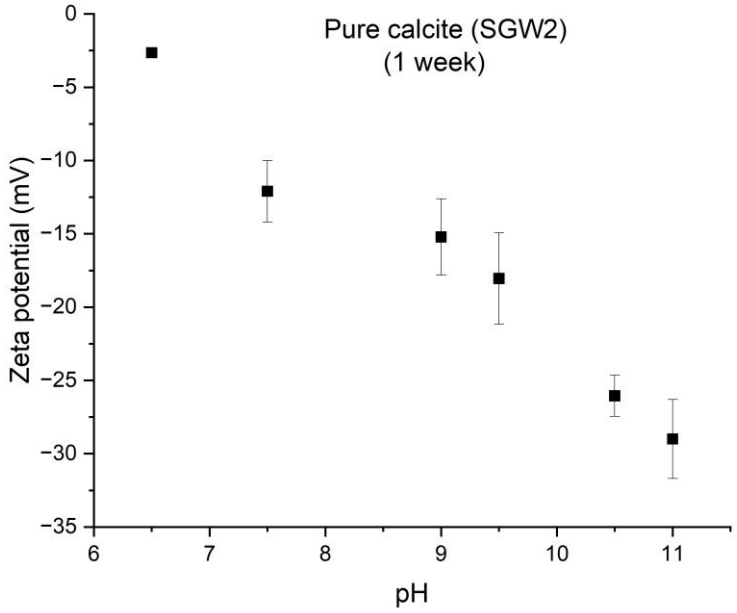

Figure 26. Series 2 Pure calcite/SGW2 zeta potential results.

Pure calcite in SGW2 appears particularly stable with pH control, even more so than in Series 1. In almost all samples there was no significant fluctuation in Ca concentration over time. Above pH ≈ 8, even the differences between aliquots from freshly prepared samples and aliquots following the first bubbling appear non-existent. None of the samples were pre-equilibrated: fresh samples were prepared for every batch in Series 2 and none reused from the previous series, undergoing the exact same procedures from the same starting point as Series 1. The only difference from the previous series was a wider range of solution pH values, which seems to have had a drastic effect.

At pH 6.5, equilibrium was clearly not achieved. Ca concentration is several times higher than in other samples and fluctuates wildly over time (Figure 25). The most likely cause for such a high concentration is calcite dissolution, as discussed in previous sections. pH 7.5 is more promising and more closely resembles the results obtained in Series 1: noticeable fluctuations can clearly be seen, but the sample appears to have centered around 20 ppm of Ca and does not deviate from it by too much.

By contrast, at pH 8.5 – 11 all samples appear highly stable. Ca concentration starts and remains low, barely fluctuating throughout the whole experiment. Even on a smaller scale (Figure 27), excluding the curve for pH 6.5, there is very little variation in Ca concentration over time. Unlike in Series 1, the samples also appear to be stable from the very start of the experiment and are missing the post-bubbling increases in concentration that were routinely seen in Figures 18-20. These differences can likely be attributed to calcite dissolving to a much lesser extent in high-pH environments, as well as the added base acting as a buffer for the carbonic acid introduced by the bubbling of CO_2 and resisting decreases of solution pH.

Greater sample stability appears to be reflected in zeta potential results as well. In Figure 26, a clear downward trend can be observed between the samples, with the zeta potential becoming more negative as the pH increases. This is in line with the theoretical assumption that the calcite surface would become more negatively charged at higher pH values due to the prevalence of anionic species in solution. An expanded pH range also aids in visualizing this trend.

As such, pH control and a larger pH range of 6.5-11 seems to have had a positive effect both on equilibration and zeta potential in SGW2. At roughly pH ≥ 8, pure calcite samples seem to become rather stable in terms of Ca concentration and equilibrate quickly, which also aids in producing more reliable zeta potential results.

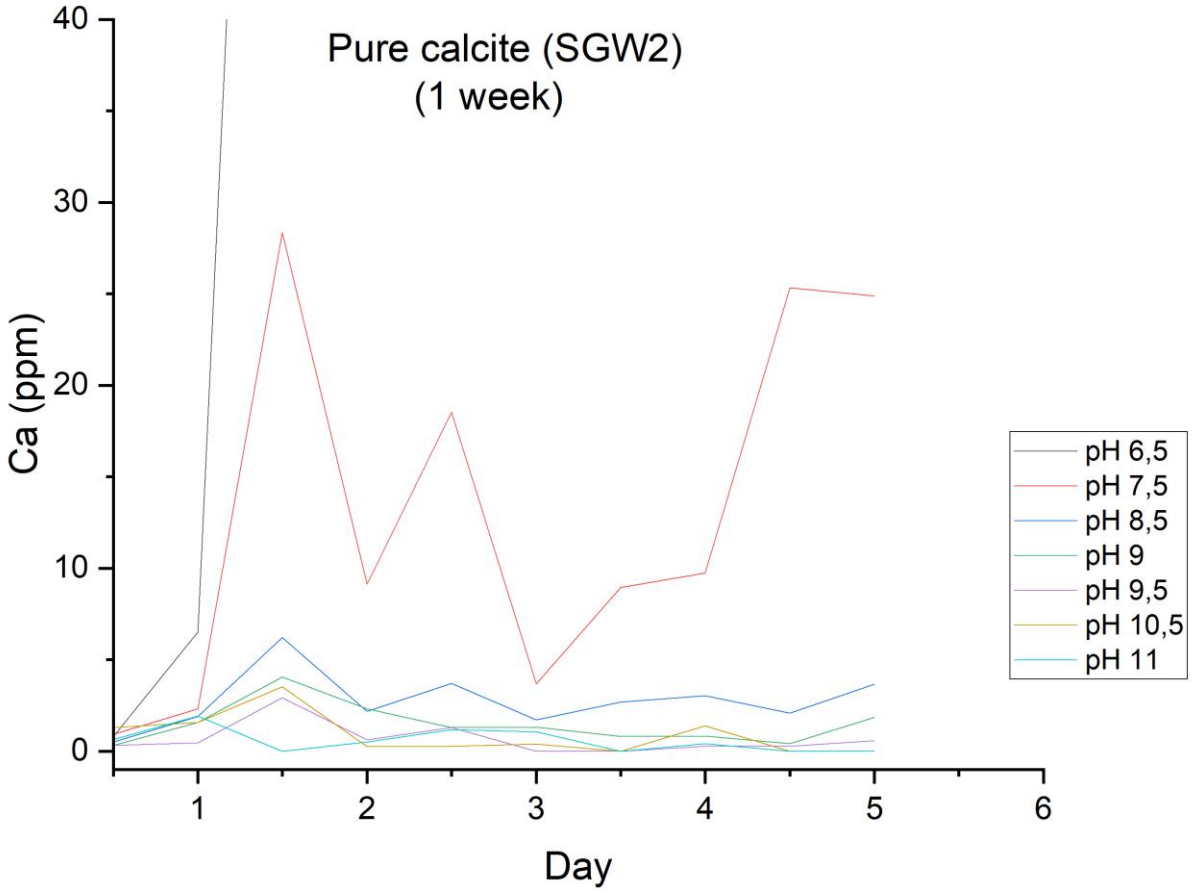

Figure 27. Series 2 Pure calcite/SGW2 equilibration results (smaller Y scale).

4.4.2 S2 Pure calcite in NaCl

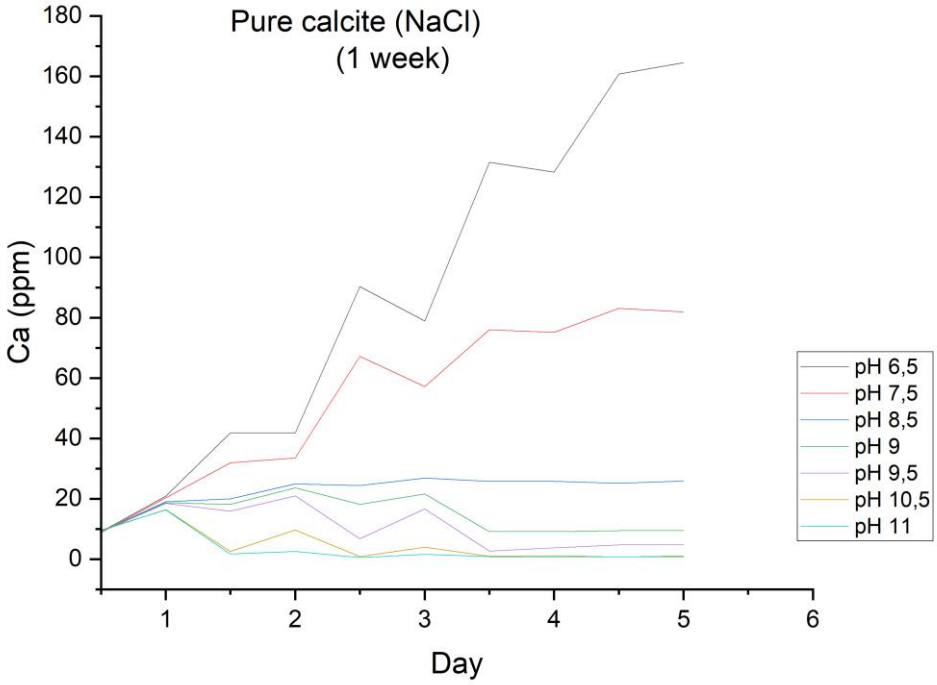

Figure 28. Series 2 Pure calcite/NaCl equilibration results.

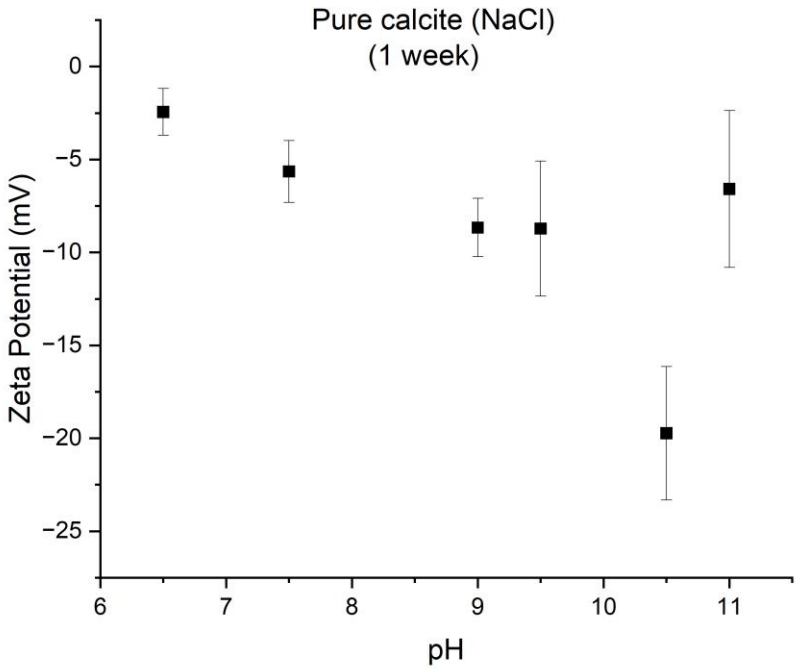

Figure 29. Series 2 Pure calcite/NaCl zeta potential results.

Pure calcite in NaCl seems to produce very similar results to SGW2. Curves in Figures 25 and 28 closely resemble each other, with only relatively minor differences between them. As shown in Figure 28, samples at pH 6.5 and 7.5 once again appear the least stable and exhibit higher Ca content than other samples, but this is much more pronounced in the case of NaCl. The sample at pH 6.5 rises to almost the same Ca concentration as in Figure 25, though this increase is more gradual. By contrast, at pH 7.5 much more calcite seems to have dissolved when using NaCl: Ca concentration is seen rising to about 80 ppm, while in SGW2 the highest recorded concentration at pH 7,5 is just under 30 ppm. Most likely for this reason the sample at pH 7.5 also appears to be far from stable, only beginning to plateau around the fifth day and clearly requiring more time than was allocated.

Similarly to SGW2, samples at pH 8.5 – 11 are much more stable. All of them remain at relatively low Ca concentrations and do not fluctuate to a notable extent during the experiment, with some of them almost looking like straight lines by the fifth day. The biggest difference from SGW2 is that the Ca content in every sample appears higher. In SGW2, all samples starting from pH 8.5 are tightly packed near 0 ppm and all remain below the concentration of 10 ppm (Figure 25). On the other hand, in NaCl the samples are spread apart far more, with several of them showing Ca concentrations close to 20 ppm (Figure 28). However, the same trend in calcite dissolution can still be observed: as pH increases, Ca content decreases, with pH 11 producing results barely above 0 ppm. In addition, all samples at pH ≥ 8.5 again appear to become quite stable over time and seem to achieve a state of equilibrium by the end of the experiment. Fluctuations in Ca concentration stop completely after the third day, coinciding with the bubbling being stopped. After this, Ca concentration seems to stay unchanged in every sample, with the only difference being that every sample stabilized around a different concentration.

The trend with zeta potentials is less clear, however. In Figure 29, while a general downward trajectory can be inferred, it is much less obvious and smaller in magnitude than the one observed in SGW2 (Figure 26). Certain samples also show results that are the opposite of what can be expected, most notably at pH 11 where the zeta potential suddenly rises significantly. Results such as these might suggest that the samples were not entirely stable and may have needed an additional few days of waiting before measurement. Alternatively, it is also possible that NaCl is inherently a less stable medium than SGW2, hinted at by greater calcite dissolution.

4.4.3 S2 Pure calcite in NaCl (5 mM) + $MgCl_2$ (2.5 mM)

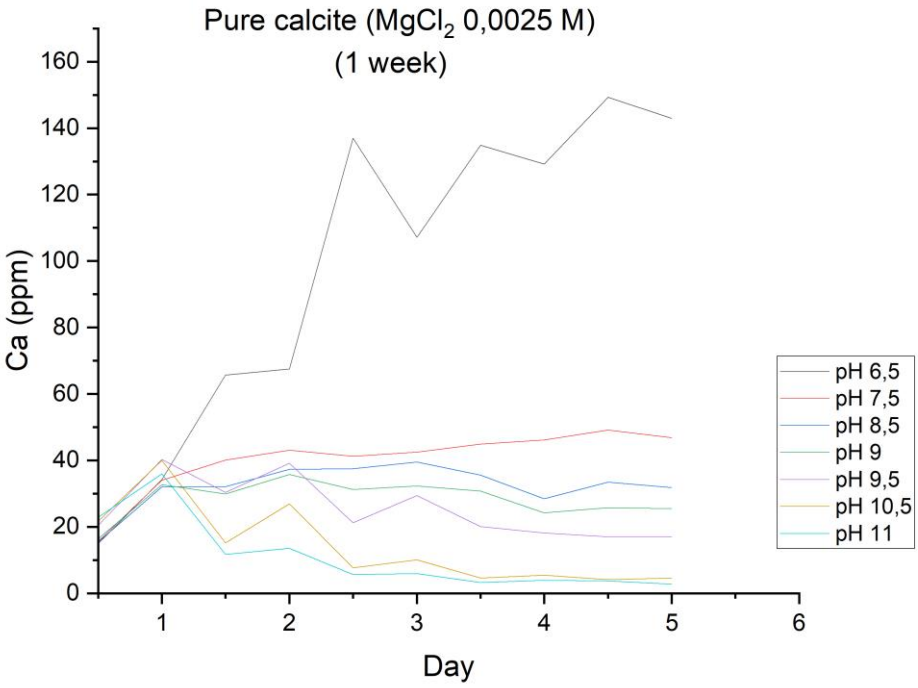

Figure 30. Series 2 Pure calcite/NaCl (5 mM) + $MgCl_2$ (2.5 mM) equilibration results.

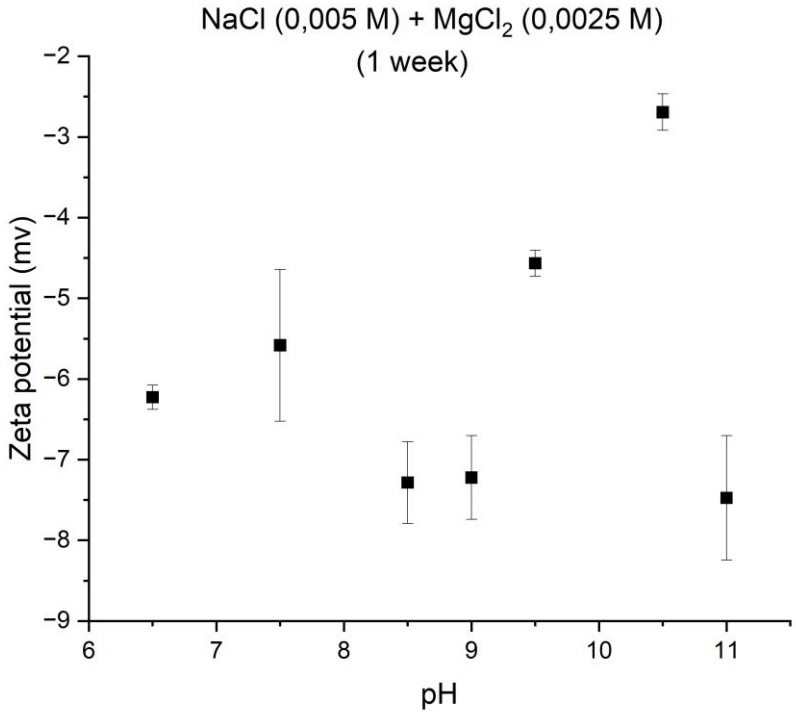

Figure 31. Series 2 Pure calcite/NaCl (5 mM) + $MgCl_2$ (2,5 mM) zeta potential results.

Pure calcite in a mixture of 5 mM NaCl and 2.5 mM $MgCl_2$ does not deviate from previously established equilibration patterns. As before, Figure 30 shows a highly unstable curve at pH 6.5 and increasing stability as pH increases. It seems, however, that in this solution the sample at pH 7.5 also managed to equilibrate rather well: fluctuations in Ca concentration are minor and the curve appears to plateau already after the first day.

Equilibration results are otherwise very similar to SGW2 and NaCl. Dissolved Ca content decreases as pH is increased, and the samples eventually become more or less equally stable and settle at different concentrations by the end of the experiment, as was seen in NaCl. It is also possible that calcite dissolution increased once again as numerous samples starting from pH 8.5 now go well beyond the previously recorded maximum Ca concentration of 20 ppm in Figure 28. At the same time, however, even though the sample at pH 7.5 still shows a higher Ca concentration than higher-pH samples, it is a notable decrease from the results seen in NaCl at pH 7.5, suggesting that a different phenomenon may have occurred instead of increased dissolution.

Zeta potential results are drastically different from previous batches. In Figure 31, the values appear randomly scattered without suggesting any sort of trend, unlike in NaCl where the beginnings of one could at least be observed. Given how the total ionic strength of this batch was kept the same as the previous NaCl batch and only difference was that $MgCl_2$ now accounted for half of it, it is likely that Mg has had a strong effect on zeta potential.

A possible explanation is the specific adsorption of metal ions to the calcite surface. As established previously, calcite readily sorbs divalent metal ions, and their complexation with charged surface groups can alter the overall surface charge to the point of switching its sign from negative to positive [7, 32, 53]. In these circumstances, the dependence of zeta potential on ionic strength also does not follow an obvious trend. Mg^{2+} is a divalent cation that is highly similar to Ca^{2+} in terms of its chemical properties, which is why it is often found incorporated into the calcite crystal structure where it can influence its growth and precipitation [54–58]. Due to these similarities, Mg^{2+} is also considered a potential-determining ion with just as much influence on zeta potential as Ca^{2+} [38]. In addition, Mg^{2+} has a smaller ionic radius than Ca^{2+} and may bind to surface groups more strongly and selectively due to reduced steric hindrance [53, 59]. As such, even though the total ionic strength of the solution in this batch was unchanged, the exact composition differed due to the presence of Mg^{2+}. As a result, it may have ended up competing with Ca^{2+} for surface sites, which could complicate surface chemistry and explain the poor zeta potential results.

4.4.4 S2 Pure calcite in NaCl (2.5 mM) + $MgCl_2$ (3.75 mM)

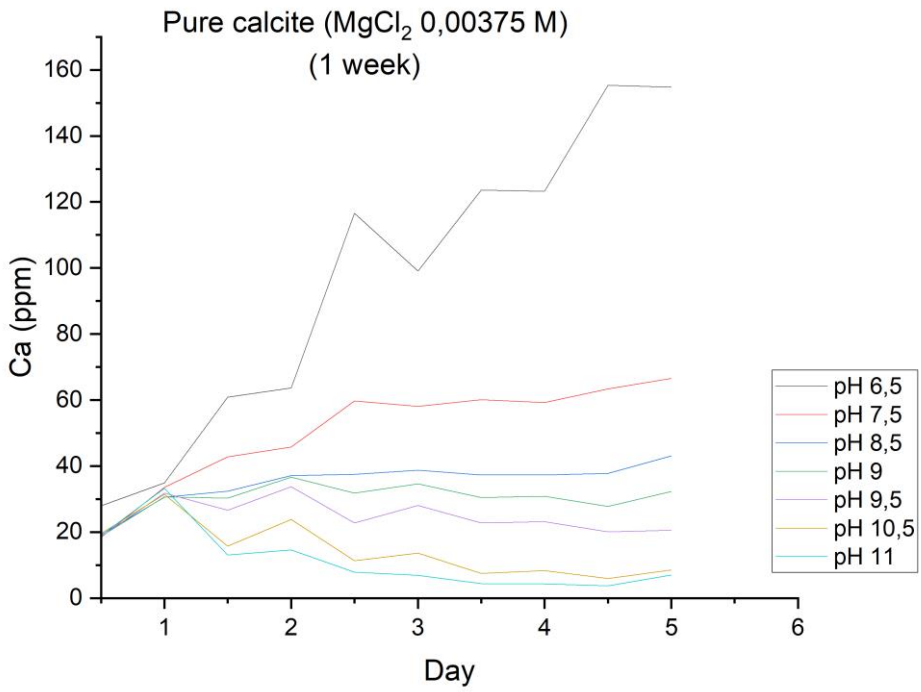

Figure 32. Series 2 Pure calcite/NaCl (2.5 mM) + $MgCl_2$ (3.75 mM) equilibration results.

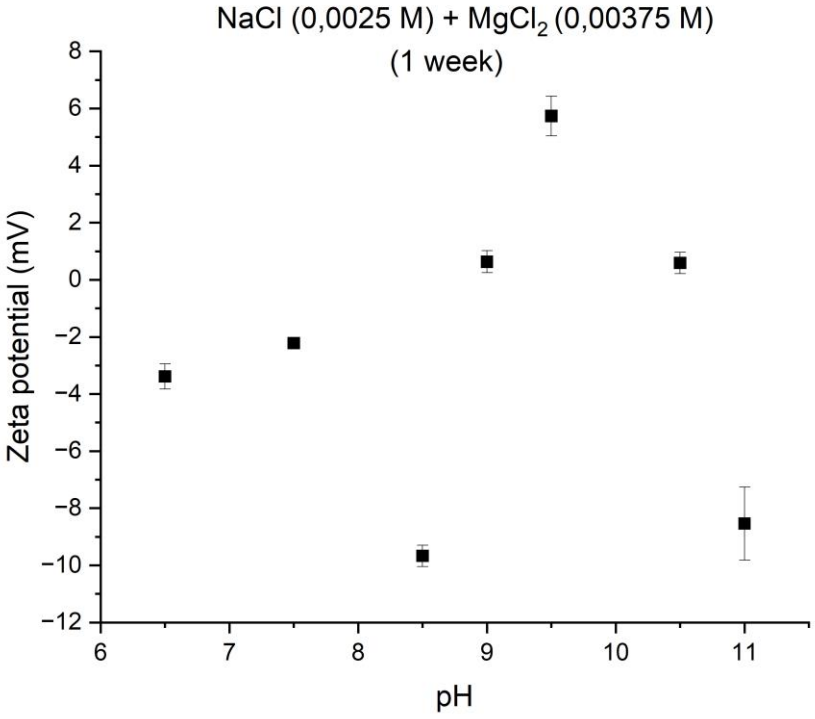

Figure 33. Series 2 Pure calcite/NaCl (2.5 mM) + $MgCl_2$ (3.75 mM) zeta potential results.

Perhaps unsurprisingly, pure calcite in a mixture of 2.5 mM NaCl and 3.75 mM $MgCl_2$ exhibits very similar equilibration patterns to the previous batch. The very same trends established in other experiments also persist: the inverse relationship between pH and Ca content is once again observed, and most samples become quite stable over time (Figure 32). The only notable difference is at pH 7.5: the sample does not seem to plateau as cleanly as the one where 2.5 mM $MgCl_2$ was used (Figure 30) and instead keeps steadily rising throughout the experiment. In addition, it reaches a Ca concentration approximately 20 ppm higher than what was seen in the previous batch. It is uncertain whether this is caused by a particular mechanism or is a result of random variation between different batches: the only variable in this case was Mg content, which seems to have had opposite effects in different experiments. The addition of 2.5 mM $MgCl_2$ seemed to noticeably decrease the Ca concentration observed at pH 7.5 compared to a NaCl solution lacking Mg (Figures 28 and 30), while a slightly more concentrated 3.75 mM $MgCl_2$ appeared to increase it (Figure 32). Nothing concrete can be concluded, however, especially since samples at other pH values seem largely unaffected by the change in Mg content.

On the other hand, zeta potential results seem to have been altered even more by the rise in Mg concentration. The same overall ionic strength as in the previous batches was maintained in this one, but the relative amount of Mg was increased further. In Figure 33, zeta potentials of different samples are once again scattered randomly, with significant differences in magnitude between even some adjacent samples. This is similar to results obtained in 2.5 mM $MgCl_2$, but with an even wider range and variation of zeta potentials. In addition, positive zeta potentials were also recorded, which never occurred in any of the previous experiments. These results make sense in the context of the previous batch, however: if Mg^{2+} complicated the surface chemistry and affected the zeta potential then, an even stronger effect can be expected if the concentration of Mg^{2+} is raised further. In this case, even more potential-determining ions would be present in solution, with ongoing sorption, desorption and complex formation. Given the occurrence of positive zeta potentials, it is also likely that some surface charges were locally altered by complexation of surface groups. As a result, it would be difficult for the system to stabilize and achieve equilibrium, leading to a random and non-representative spread of zeta potentials. Mg^{2+} thus appears to be highly detrimental to zeta potential measurements, and its presence should be avoided.

4.5 Series 3 Equilibration

Below are the MP-AES and zeta potential results from the third sample batch (only pure calcite). Both batches are a direct continuation from Series 2: the exact same samples were studied for an additional month after the original 5 days of equilibration.

4.5.1 S3 Pure calcite in synthetic groundwater (SGW2)

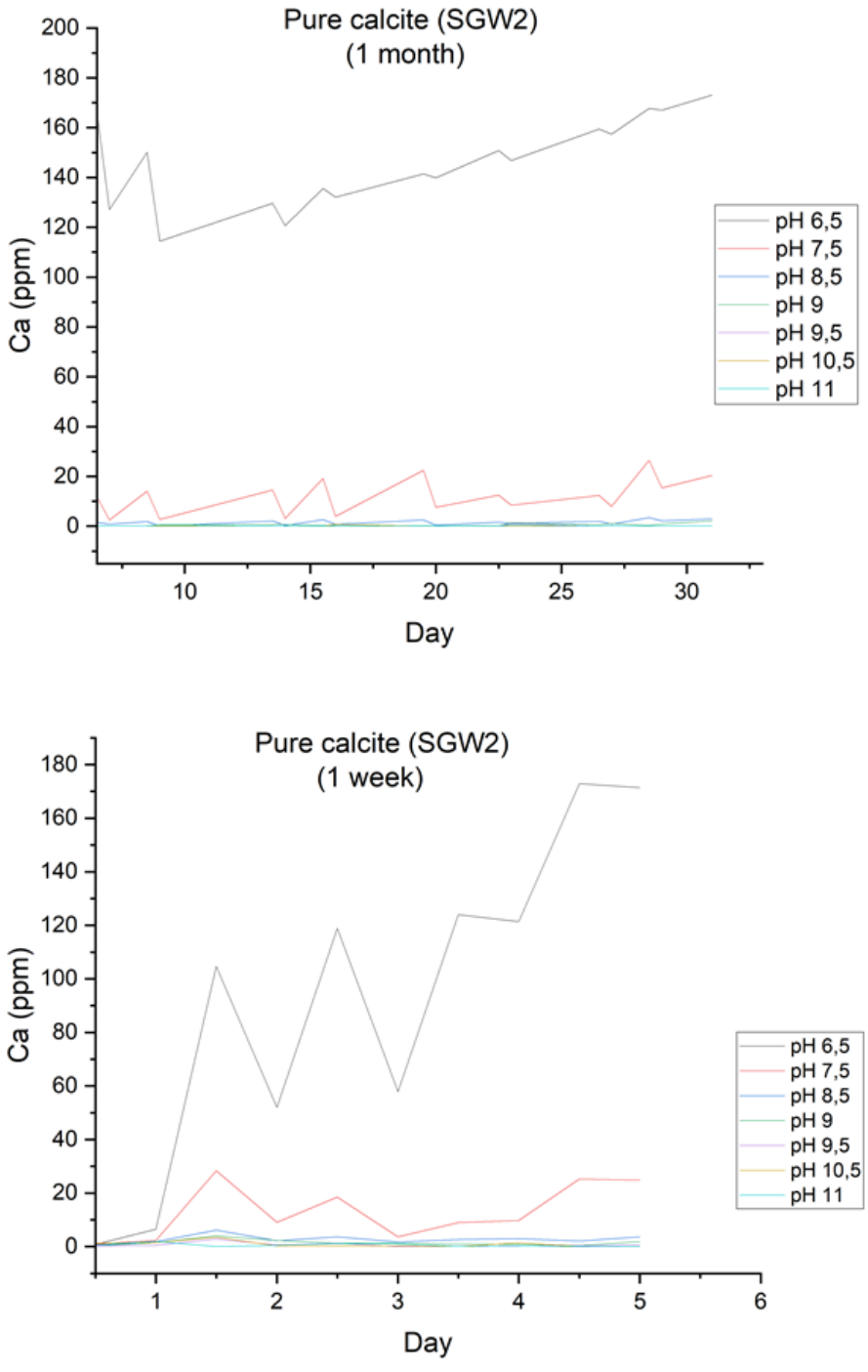

Figure 34. Series 3 Pure calcite/SGW2 equilibration results and comparison with 1 week.

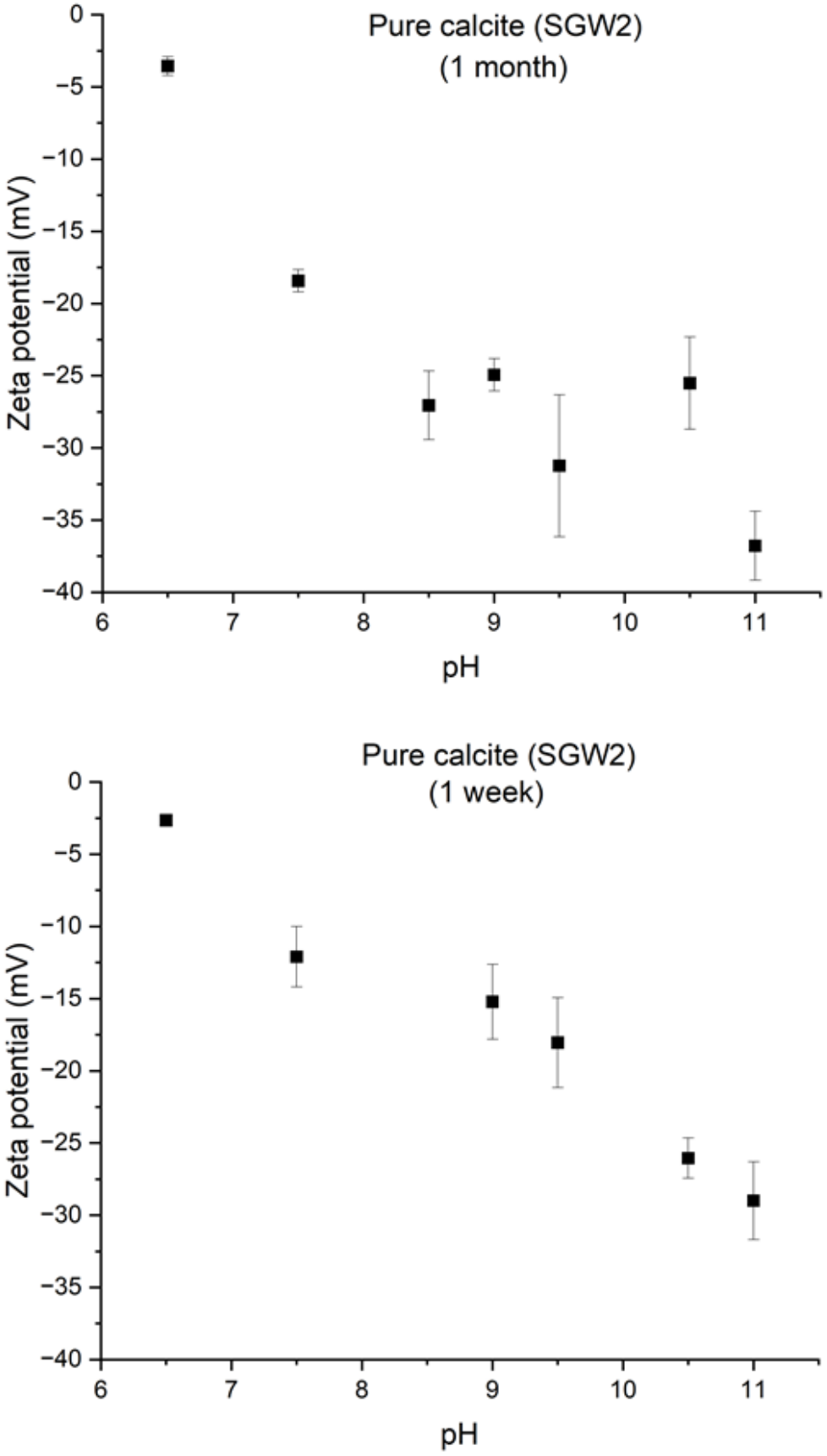

Figure 35. Series 3 Pure calcite/SGW2 zeta potential results and comparison with 1 week.

Pure calcite in SGW2 appears to maintain a steady equilibrium when monitored for an additional month. In Figure 34, at pH 6.5 the sample is still highly unstable for the entire duration of the experiment and exhibits significantly higher Ca concentrations than any other sample. pH 7.5 appears to be right on the verge of equilibrium: the curve is trending towards a straight line, although noticeable fluctuations in concentration remain. At pH 8.5 and above, the samples appear to be at an effectively constant Ca concentration, with the most significant fluctuations being approximately 1-3 ppm in magnitude (Figure 36). In addition, beyond pH 9 Ca concentration remains very low and rarely exceeds 1 ppm. When approaching pH 11, most of the results were under the MP-AES' detection limit. As such, high pH again appears to have significantly reduced the dissolution of calcite and contributed to sample stability. It is also unlikely that the results would change to any notable extent if the experiment were conducted for even longer: over the course of one month most of the samples appear to have settled around a certain Ca concentration and show no signs of significant variation or any new developing trends. The more unstable samples seem to have been influenced most by pH and would not benefit from longer equilibration times.

Zeta potential results are also very similar to Series 2. Compared to Series 2 results, the trend in Figure 35 is not as obvious but still exhibits a clear downward trajectory. In addition, more negative zeta potential values than before are reached at higher pH, possibly due to a longer experiment time stabilizing the samples more and allowing calcite surfaces to adsorb more of the anions present in solution. This difference is rather small, however, and variation in zeta potentials could just as easily be attributed to random errors and instrument imprecision.

Overall, extending the equilibration time from one week to one month does not seem to have had any significant effect on pure calcite in SGW2. All samples seem to equilibrate as well as possible during the first few days of the experiment and simply maintain their respective Ca levels afterwards regardless of how long the equilibration is continued. In addition, it does not seem possible to equilibrate samples below pH 8: calcite dissolution and precipitation lead to highly variable Ca concentration, which does not settle even after one month.

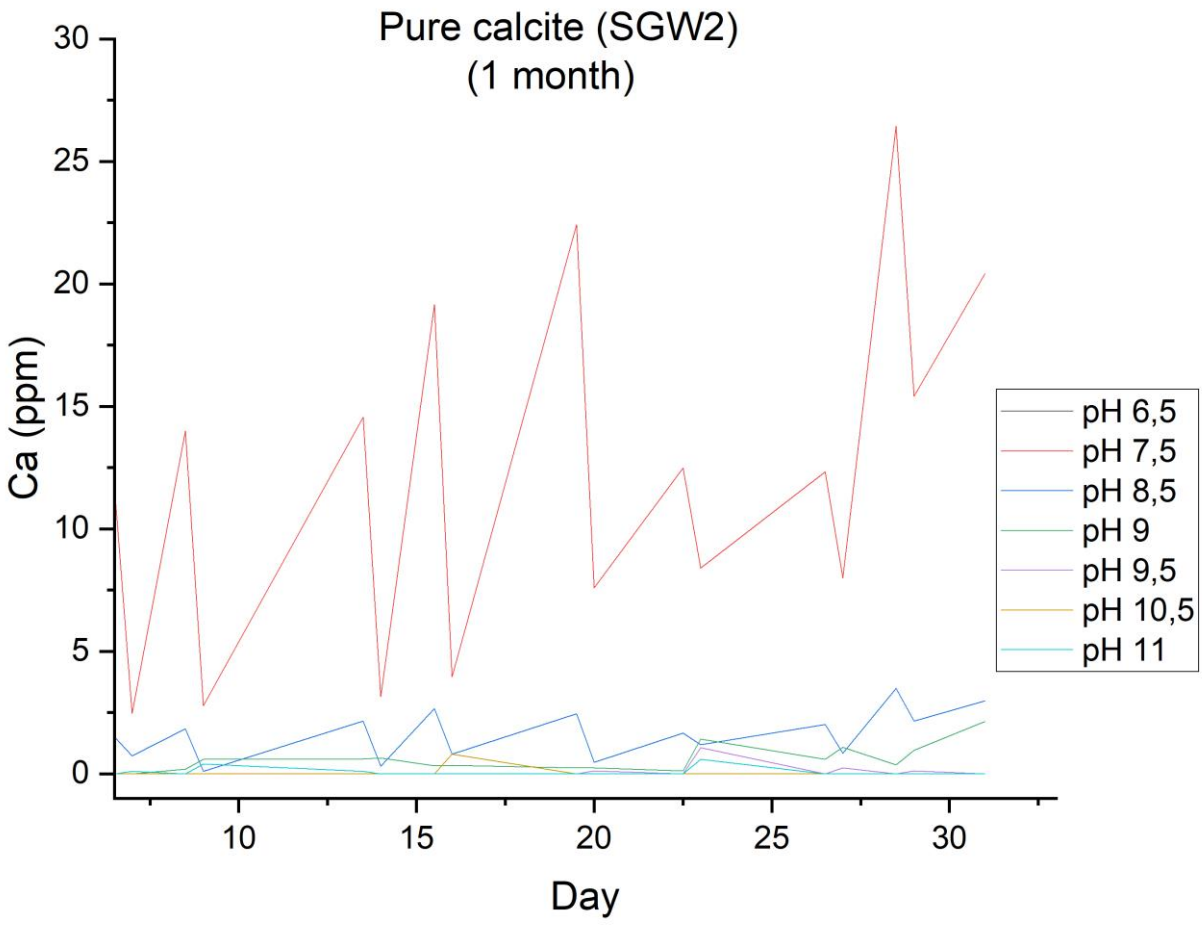

Figure 36. Series 3 Pure calcite/SGW2 equilibration results (smaller Y scale).

4.5.2 S3 Pure calcite in NaCl

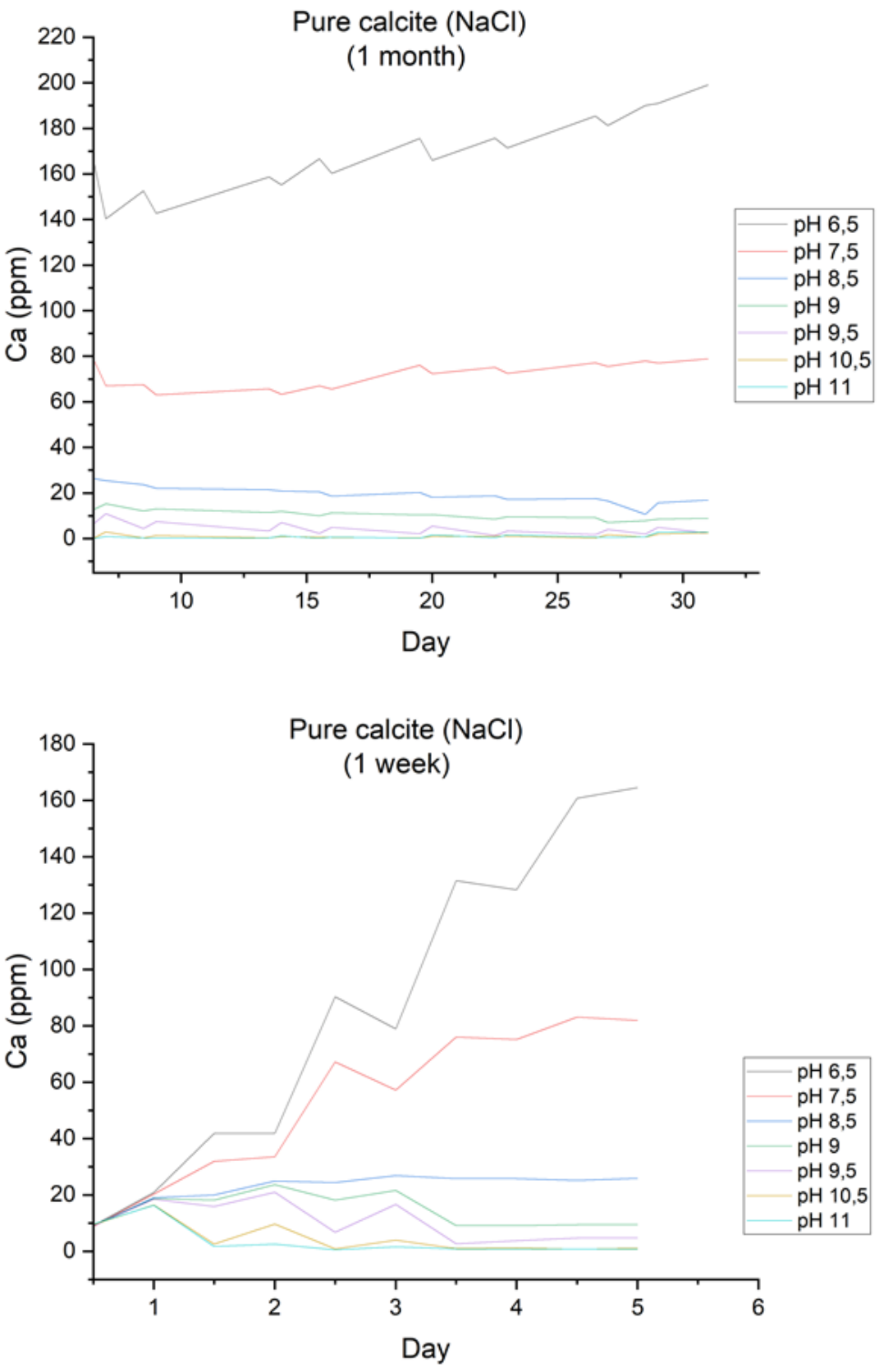

Figure 37. Series 3 Pure calcite/NaCl equilibration results and comparison with 1 week.

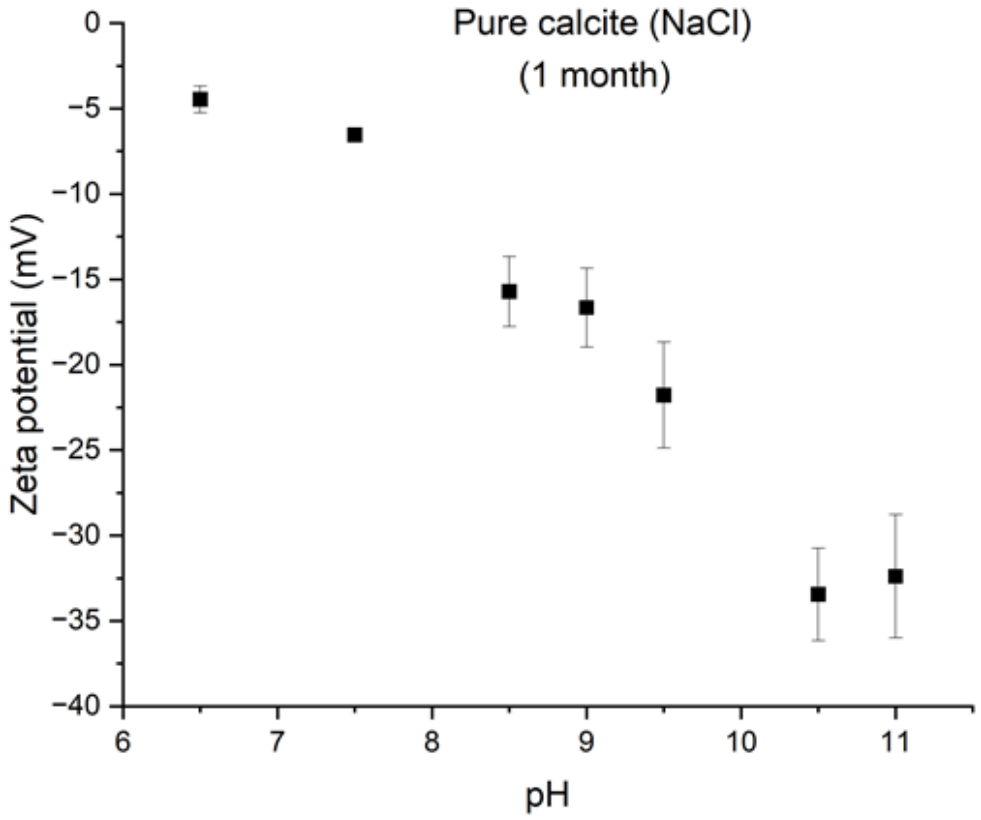

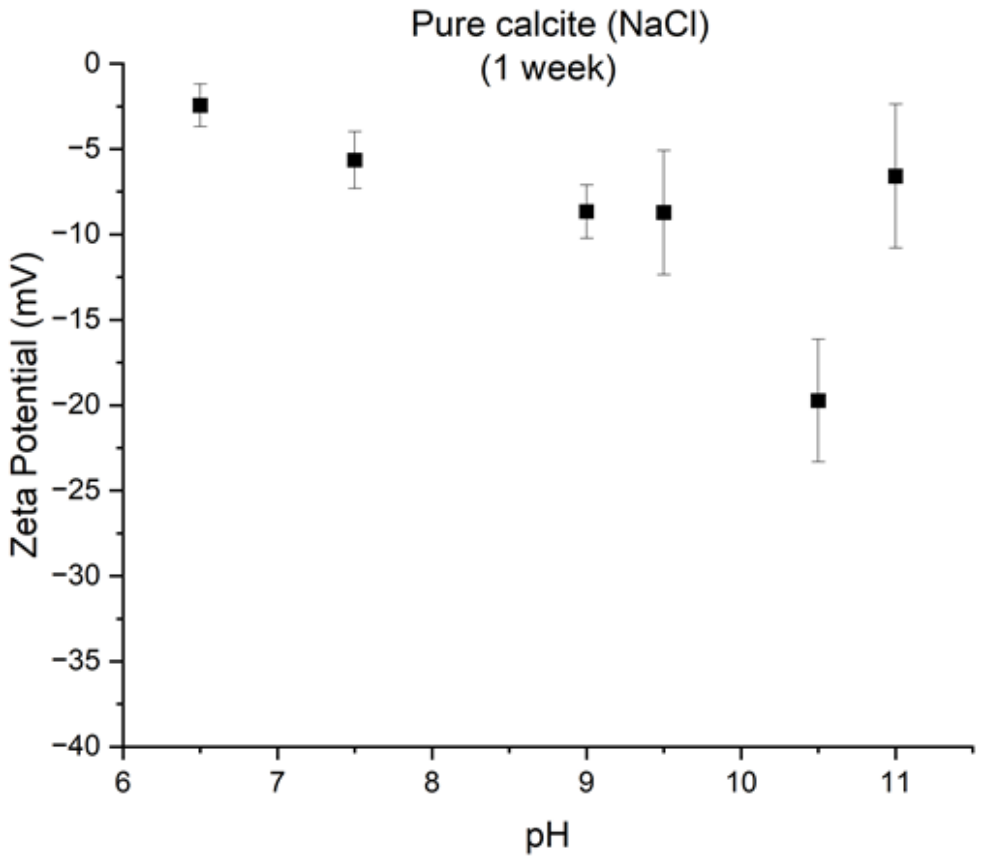

Figure 38. Series 3 Pure calcite/NaCl zeta potential results and comparison with 1 week.

Pure calcite in NaCl also appears to maintain its equilibrium over the course of one additional month of study. For the most part, Figure 37 simply continues the trends established in Series 2, and no improvements to sample stability can be observed. High-pH samples have effectively plateaued already during Series 2 experiments, with only small and irregular fluctuations in Ca concentration still occurring. At pH 6.5 the sample still fails to equilibrate, and a rising trend in Ca concentration is seen even after one month. The only notable difference from Series 2 is pH 7.5: while the sample was clearly not yet stable in Series 2, after an additional month of equilibration it appears to finally plateau in Figure 37. While Ca concentration at pH 7.5 is still much higher than in higher-pH samples, by the end of the experiment it seems only slightly less stable than in them. As such, while pH clearly has the most influence on equilibration, in this case a longer equilibration time seems to offer a small benefit by allowing lower-pH samples to stabilize better.

Zeta potential results appear much improved from before. Compared to Series 2, Figure 38 shows a much clearer trend towards more negative zeta potentials as sample pH increases. In this case, the difference is also unlikely to be caused entirely by random factors such as errors: the data points are arranged with a much clearer trajectory, changes in magnitude between individual zeta potentials are more noticeable, and much more negative zeta potentials are reached. Nearly all Series 2 results remained above -10 mV, and overall were quite close to each other in value. By contrast, Figure 38 shows a much more evident decrease in zeta potential as a function of sample pH after one month, and the lowest recorded potential at the highest pH values approaches -35 mV. As such, a longer equilibration time seems to have been very beneficial to zeta potential measurements.

Overall, extending the equilibration time by an additional month seems to have improved the results in the case of pure calcite in NaCl. While no significant difference was observed in terms of equilibration, there is a very clear difference between zeta potential results obtained after one week and after one month, possibly due to calcite surface chemistry becoming more pronounced and established over time. This could also suggest that Ca concentration is not ideal as an indicator of equilibrium. There does not seem to be a strong correlation between it and the quality of zeta potential results: even if the Ca concentration appears remarkably stable and unaffected by the length of equilibration, this does not necessarily mean that zeta potential will be similarly unaffected, as shown in this sample batch.

4.6 Equilibration with CO_2 compared to exclusion of CO_2

In an earlier work, calcite zeta potential was determined under anoxic conditions, with both O_2 and CO_2 excluded from the atmosphere [33]. The work was done in a glove box with a constant N_2 atmosphere, where calcite samples were placed in a 0.01 M $NaClO_4$ solution and shaken over the course of two days. Sample pH was controlled on both days of the experiment, and zeta potentials were measured directly afterwards. As such, it is a very similar procedure to the one described in this work: equilibration with pH adjustment was attempted for the exact same types of calcite in an equilibration solution that, in terms of zeta potential, is effectively equivalent to NaCl that was used in this work. The two main differences are the length of equilibration and the atmosphere that the samples were exposed to. Only 2 days were allocated to equilibrating the samples as opposed to a minimum of 5 in this work, and the influence of CO_2 was controlled with essentially the opposite approach: instead of saturating the samples, they were instead kept completely isolated from the gas. Results from this work are presented in Figure 39.

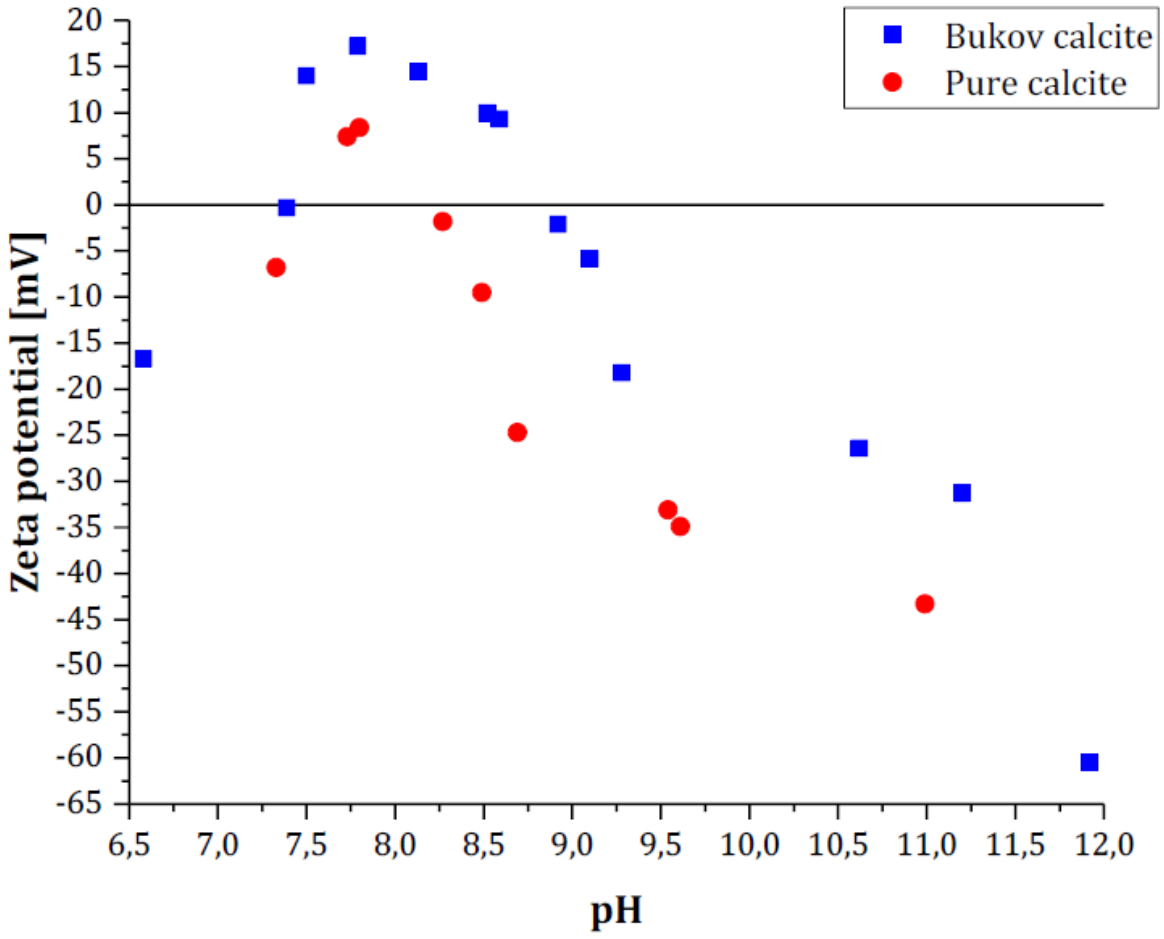

Figure 39. Calcite zeta potentials under CO_2 exclusion in $NaClO_4$ [33].

The most direct comparisons that can be made between this work and the anoxic work relate to Bukov and pure calcite in NaCl, summarized in Figure 40.

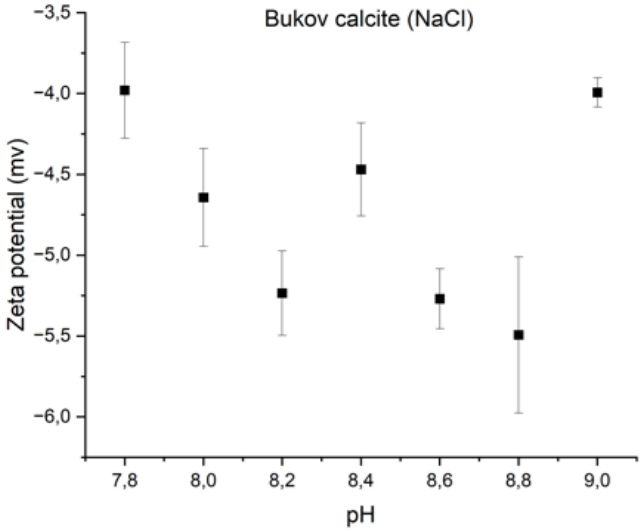

Figure 24. Series 1 Bukov calcite/NaCl zeta potential results.

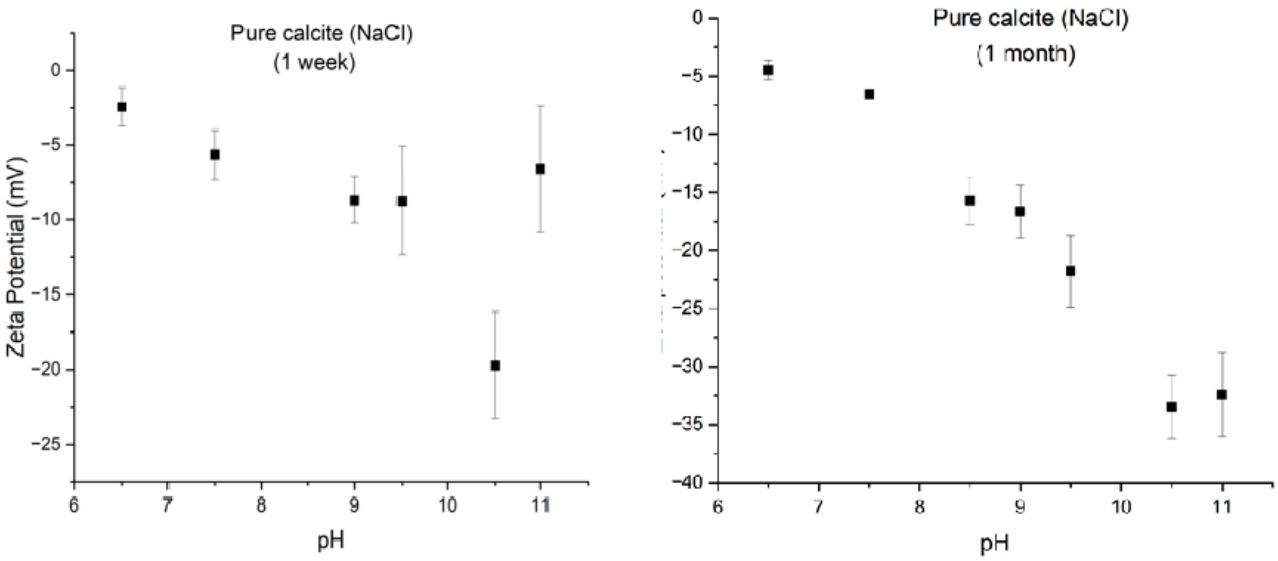

Figure 29. Series 2 Pure calcite/NaCl zeta potential results.

Figure 40. Zeta potentials of CO_2-equilibrated calcite in NaCl.

In Figure 24, it is worth noting that the pH range is only 7.8 – 9 as opposed to 6.5 – 12 in Figure 39. Significant differences can be seen in this interval, however. In Figure 39, almost all zeta potentials for Bukov calcite between pH 7.8 – 9 are positive: in this work, all potentials remained below 0 mV, and no gradual rise or subsequent decrease in zeta potentials can be observed. The lowest zeta

potential recorded in this work at pH 8.8 closely mirrors the value observed at pH 9 in Figure 39, but that is the only similarity between the results.

Figure 29 is more similar to Figure 39. Comparing to pure calcite this time, and with almost the same pH range of 6.5 – 11, the most obvious difference is the lack of positive zeta potentials in Figure 29 while they can be clearly observed in Figure 39 around pH 7.7. Every value in Figure 29 again remains below 0 mV, although above pH 8.5 zeta potentials in Figure 39 reach much more negative values than any that are seen in Figure 29. Ultimately, however, both figures exhibit a fairly clear downward trend in zeta potential with increasing pH, with the biggest difference being the region of positive zeta potentials present in the anoxic work.

Figures 38 and 39 resemble one another the most. Every zeta potential in Figure 38 again remains under 0 mV, and there is no region of positive potentials or even the slightest rising trend like the one seen in the anoxic work. Instead, the data points in Figure 38 are arranged like the points in Figure 39 above pH 8.25: a clear downward trajectory towards increasingly negative zeta potentials can be seen as pH increases. However, more negative zeta potentials are again reached in the anoxic work: the lowest recorded value in Figure 38 is around -35 mV, while Figure 39 reaches roughly -45 mV.

In general, there appears to be one main difference between this work and the one performed under an N_2 atmosphere. Under the exclusion of CO_2, a region of rising zeta potentials was always observed around pH ≈ 7.5 – 8, crossing over into positive values before falling back below 0 mV as pH increased. This phenomenon was not observed in this work: all zeta potentials remained negative and only decreased further along with rising pH. The cause of positive zeta potentials is not known for certain as they could have been a result of impurities present in the solution, incomplete equilibration or some unknown factor. However, given their absence in this newer work, it is possible that incomplete equilibration may have been the cause. As discussed previously, zeta potentials can be negative at low pH values due to calcite dissolution and the loss of ions from its surface, which can be seen between pH ≈ 6.5 – 7.5 in Figure 39 [35]. As pH increases, dissolution is reduced, stabilizing the system. However, at pH ≈ 8 neither anions nor cations are particularly favored by solution conditions, making them compete for surface sites. As such, if the system is not in equilibrium it may be possible to observe positive zeta potentials when approaching this pH if more cations happened to be adsorbed on the calcite surface at the time of measurement. This may explain the regions of positive zeta potentials observed in Figure 39. On the other hand, since this

newer work specifically set out to equilibrate calcite samples with CO_2 through direct exposure and allocated additional time to this procedure, the samples may have equilibrated better and experienced more stable conditions by the time of zeta potential measurements. As a result, all zeta potentials remained negative and exhibited a downward trend with increasing pH. The same trend is also observed in Figure 39, but only above pH ≈ 9, at which point anionic species in solution likely became dominant and could reliably displace positively charged ions from the surface.

5. Discussion and improvements

This work set out to investigate the possibility of equilibrating calcite samples by direct saturation with CO_2 and the effect this has on the calcite surface charge and zeta potential. While new information has been gained, numerous improvements can still be made to the procedure for future experiments.

5.1 Environment and atmosphere

The most immediate issue concerns the environment of the experiment. As mentioned previously, the samples would ideally be placed in an isolated environment with a controlled atmosphere so that they could stabilize over time. Changing conditions and exposure to air could result in the uncontrolled dissolution of atmospheric CO_2 and the entry of other possible contaminants [18, 32]. This would result in the amount of potential-determining ions changing, affecting surface reactions and rendering zeta potential measurements unreliable. Carbonate concentration almost certainly did not remain stable, however, as the samples could not be kept under a constant and controlled atmosphere.

While the original plan was to simply store all samples inside a glove box with a constant pCO_2 and allow them to equilibrate, this proved impossible due to a number of practical concerns. To begin with, the length of the experiment under these conditions was projected to be prohibitively long: several months would be needed in order for the CO_2 to dissolve and properly saturate the samples. In addition, no vacant glove box with the capability of controlling its own atmosphere was available in the first place. None could be repurposed and committed to housing a specific CO_2 mixture for the length of time that this work would require, making it necessary to use a much simpler model (Figure 14). This model amounted to little more than a sealed plastic box that had to be manually filled with gas from an external bottle. While this could theoretically meet the requirement of having

a constant atmosphere, in practice the integrity of this glove box was highly questionable, and some gas exchange with the surrounding air must have constantly occurred.

On top of an unreliable internal atmosphere, the glove box was also of insufficient size. Opening and repressurizing this particular glove box would significantly disturb its interior atmosphere each time this was done, meaning that in addition to the samples, every object necessary for the experiment would have to be stored inside the glove box as well to avoid having to open it after starting the experiment. This would have to include hundreds of centrifuge tubes for every single aliquot that was to be taken during those months, in addition to items like tube racks, pipettes, pipette tips, a pH meter, deionized water, acids, bases, waste bags and solution containers, to name a few. These items simply could not fit inside the glove box without making it impossible to do any work in it. In addition, the glove box lacked any access to power for the pH meter, and no reasonable number of portable chargers could last long enough to cover the entire experiment, rendering pH monitoring impossible. Lastly, even a single sample batch along with the necessary items filled up the glove box to an alarming extent, meaning that a very limited number of samples could be processed in this way simultaneously. Considering the months-long timescale, this would either drastically cut down the number and types of samples studied in this work, or extend the experiment by possibly years.

As such, the main limitation of this work was the lack of a suitable environment to conduct it in. If a proper glove box with the appropriate size, access to power and capability to maintain a stable atmosphere were available, this issue and most of the following issues could have been avoided entirely.

5.2 Bubbling setup

Because of the slow speed of passive dissolution and size limitations of the glove box, the initial idea of constant pCO_2 was abandoned. Instead, direct bubbling of a 250 ppm CO_2/N_2 mixture into the samples was chosen as a way to more quickly introduce CO_2 to the samples and speed up its dissolution. However, because this was never part of the original plan, there was no dedicated infrastructure or equipment available, making it necessary to utilize simple and custom-made solutions with questionable reliability.

The first issue with this method was the lack of any way to introduce the gas into the samples. A dedicated delivery system simply did not exist due to a lack of any previous demand, and it was

deemed too costly and wasteful to invest in one for the purposes of this work alone. As a result, a simple solution was chosen, essentially being nothing more than a series of flexible plastic tubes connecting the gas supply to the samples (Figures 13-17). These tubes were measured and cut to be roughly of the same length at each stage, but this was done by hand and thus none could be made exactly identical. While sufficient, this resulted in poor repeatability for the experiment as the exact conditions are effectively impossible to replicate by anyone else.

The custom nature of the delivery system also had an effect on its performance. Gas would naturally flow along the shortest and clearest path, meaning that ideally every part of the system should be identical to divide the flow evenly. However, because every part of the tubing was made and assembled by hand without any special tools or materials, there inevitably were small differences between them. Most prominently, the length of the tubing varied, and gas would preferentially flow along the shorter paths more readily than the rest. This had unfortunate implications for the bubbling because at the end of its path and upon encountering the solution, the gas would have to break through surface tension in order to reach the sample. Since gas flow along certain paths was stronger than in others, it was not distributed equally and would struggle to overcome surface tension in some samples while flowing reliably into others. This issue could be resolved by increasing the overall gas flow until it was strong enough in all parts of the system, but this also occasionally resulted in samples being disturbed to the point of spilling over if they already had a strong enough gas flow originally. As a result, bubbling could not be a slow and controlled process and was instead quite violent and unpredictable. In addition, this naturally accelerated the expenditure of the gas mixture, which led to its own problems.

The most significant issue with the 250 ppm CO_2/N_2 gas mixture was that it was quite expensive and could not be used anywhere outside of this work, making it highly wasteful to acquire and store in large quantities. As a result, its supply was limited and its use had to be minimized as much as possible, which was made difficult by the need to overcome flaws in the gas delivery system by using faster flow rates. In addition, concerns about cost made it necessary to make further revisions to the plan. Initially, the intention was to bubble the gas constantly over a period of several days, essentially exposing the samples to a constant pCO_2 more directly and locally rather than relying on passive dissolution from the environment. However, it was discovered that at the flow rates necessary to reliably deliver the gas, a single bottle would only last a little over two days at best. Due to the high cost of replacement and the large number of samples to process, it was instead

decided to only bubble the gas in one-hour-long sessions. At other times, the samples were tightly capped to minimize their exposure to outside environments and maintain a constant internal pCO_2 that they achieved after bubbling. As such, the specialized nature and high cost of the gas meant that it could not be used to the fullest extent possible, which likely had a negative effect on equilibration.

In addition, gas delivery imposed a limitation on sample size. As stated previously, dividing the gas among different delivery tubes weakened the flow heading towards each individual sample, and this flow would sometimes be unable to overcome surface tension when it encountered the solution. The only way to counteract this was to increase the total flow rate, which ran contrary to the need to minimize gas expenditure. As a result, increasing the number of samples being bubbled simultaneously effectively meant increasing the use of gas and thus driving up costs, making it necessary to reach a compromise between a sufficiently large sample size and acceptably low gas expenditure. This is the reason why samples had to be processed in individual batches, and why no more than 7 samples were ever processed at a time. In turn, this limited the number of data points obtained from each experiment and extended the duration of the work considerably as it was impossible to process large quantities of samples simultaneously even if there would otherwise have been opportunity to do so.

Overall, the lack of specialized equipment gave rise to most issues with the bubbling system. The use of simple materials and non-uniform parts resulted in unequal gas delivery to the samples, which necessitated the use of higher flow rates to overcome the issue. This meant that an expensive gas mixture would be expended more quickly, which in turn limited the time it could be used for, reduced the number of samples that could be processed, and made it difficult to properly expose the samples to the gas. Ultimately, the bubbling setup, while functional, contained numerous flaws that often gave rise to other flaws that all fed into each other. The only sensible improvement to make would be to use a dedicated gas delivery system and not limit the use of the gas mixture, but the feasibility of these improvements depends entirely on the available budget.

5.3 Exposure to air

As mentioned previously, all samples should ideally have been stored in an isolated environment with a constant atmosphere, which could not be achieved. A simple glove box was used over the course of this work, but because of the bubbling it could not be sealed or pressurized. Due to a design limitation there was no way to connect an additional tube to the glove box, and the gas

delivery tubing had to enter through a separate opening that was not designed for that purpose. This opening was originally connected to the ventilation system through a filter and used to manually vent excess gas without compromising internal atmosphere. Following this modification, excess gas would eventually still exit through that same opening, but it could no longer be sealed due to having a gas tube passing through it, leaving the glove box constantly open to the atmosphere. As a result, the glove box essentially contained regular laboratory air at all times, and the only reason it was still used at all was that it provided a convenient location to conduct the experiments.

This marks the primary issue facing the samples: while exposure to air was to be avoided completely, it was inevitable with the setup used in this work. Sample tubes had to be open to the atmosphere during bubbling to allow excess gas to escape, and while it can be assumed that the CO_2/N_2 gas mixture would displace anything dissolving from the air during bubbling, this could not be kept constant due to high costs. An internal atmosphere inside the glove box could not be created using this gas mixture either as the way the gas entered also kept the glove box permanently open to the outside atmosphere. The gas was also too expensive to use in this way regardless, which is also why the glove box's original tubing could not be replaced to fill it with this particular gas instead to keep air out between bubbling sessions. As such, it is very likely that the samples experienced some form of contamination at times when they were not capped and not undergoing bubbling. While efforts were made to minimize the time of exposure, it is unknown how well the samples were isolated from air since the only measure that could be taken to do so was to cap the tubes immediately after bubbling concluded. It also cannot be known for certain how well one hour of bubbling truly saturated the samples with CO_2 and how well they maintained their concentration between sessions. Lastly, the samples were always sealed in an environment that contained regular air, meaning some of it would always be trapped inside the sample tubes regardless even after they were capped for storage.

Exposure to air was not limited to the glove box either. Due to relatively high gas flows, bubbling was always rather active and disturbed both the sample solution and the solid calcite at the bottom, creating a suspension. Aliquots could not be taken from such samples, and they regularly had to be brought out of the glove box for centrifugation. Similarly, pH could not be recorded inside due to a lack of a power supply, and samples had to be measured outside. Naturally, this meant opening the tubes and leaving them open to laboratory air for extended periods of time while measurements

were ongoing. In addition, pH adjustments had to be done at this time as well, further extending the time each sample spent open and exposed.

In the confines of this work no alternatives were available, and some exposure to air had to simply be accepted and its possible effects taken into account. The only realistic way to combat these issues would be to use a proper glove box, as mentioned previously, since a lack of such is what led to these flaws in the first place.

5.4 pH adjustment

pH adjustment was also a likely source of error. While a set pH range with specific increments was chosen, there was no way to predict how much acid or base must be added to any sample and in what concentration to reach the desired values. In addition, samples would not maintain their respective pH values and needed constant monitoring and adjustment to avoid drifting too far. HCl and NaOH had to be added regularly and essentially blindly until a reasonably extensive record of amounts added to each sample could be created and rough trends established. Because of this, pH adjustment was a very time-consuming process that consisted of alternating between measuring pH and adding HCl/NaOH until an acceptable value was achieved for every sample. This not only slowed down the experiments in general, but also forced the samples to be exposed to air for even longer while they were being measured. This was made even more problematic by the fact that sample pH did not behave predictably or have clear trends: sometimes a sample could maintain an almost identical value overnight and need no adjustment, while at other times the same sample could drift and require significant adjustment to shift even a little.

In addition, not all pH values were realistic to reach. For instance, pH 6.5 is unlikely to have lasted in any sample: in almost every case pH increased to around 8 overnight even if the sample was left undisturbed after adjustment. The same happened even if pH was adjusted to much lower values such as 4 the previous day, meaning it was not possible to pre-emptively compensate for the increase by intentionally changing pH to a lower value than the true desired one. It appears that at a low enough pH calcite dissolution would always begin, and the subsequent reactions would always return the sample to the lowest possible stable point. The same phenomenon was observed with samples at pH 7.5, albeit to a lesser extent. At higher pH values, samples were significantly more stable but still could not maintain a truly constant pH, regularly requiring unpredictable and slow adjustment. As such, it is worth noting that the pH range targeted in this work was not fully attained, and achieving the desired pH also had to be balanced with maintaining sample equilibrium. Zeta

potential measurements could not be conducted immediately after pH adjustment as the calcite surface required time to regain equilibrium after the addition of acid or base, but they could not be delayed too long either as pH would drift further away from the desired values over time. Because of this, some variation was present in every sample, and below pH = 8 it cannot be stated with any certainty if the samples even maintained the indicated pH by the time their zeta potentials were measured.

The impact of the addition of HCl and NaOH may also be worth considering. For the most part, only small amounts were needed to adjust pH, which should have little to no effect on the sample aside from changing the pH. However, because adjustment had to be performed regularly over the course of a week and all the way up to a full month in some cases, these small amounts could potentially add up and become significant. In the case of certain samples, volumes of over 1 ml of acid or base were sometimes needed to reach the desired value during only one adjustment, which is not a negligible amount in a 50 ml sample. In certain cases, even 1-2 M acid/base solutions had to be used because less concentrated acids and bases proved insufficient and would exceed the maximum volume of sample tubes with continued addition. Furthermore, the ionic strength of equilibration solutions was intentionally kept low for the sake of zeta potential measurements, which would only strengthen the impact that added ions could have. Na^+ and Cl^- were originally present in most equilibration solutions, but their amounts would grow over time due to the addition of HCl and NaOH, making it difficult to judge the true ionic strength and composition of the solutions. While ions like Na^+ and Cl^- are generally thought to have little to no tendency to sorb onto the surface of calcite and considered indifferent, zeta potential is known to decrease in magnitude with increasing ionic strength, which indifferent ions do contribute to [38, 60]. Because of this, zeta potentials could possibly begin to be affected if an experiment lasts for a long enough time as the equilibration solution could gradually change from its starting state and experience an increase in its ionic strength.

Given the importance of pH to zeta potential, these issues may not have an easy or obvious solution. Adjustment is necessary to create a wide enough range of values, and there is little that can be done about the unpredictable nature of sample pH. As such, the addition of extra ions to the solutions and the slow and uncertain process of pH adjustment may be inherent flaws and sources of error that have to be accepted. Fortunately, due to being monovalent ions, Na^+ and Cl^- are much less likely to influence the zeta potential of calcite than ions such as Mg^{2+} regardless. It may, however, be

worth setting the lower boundary of experiments at around pH = 8: below this point calcite samples appear highly unstable and their pH becomes too unpredictable to reliably achieve any particular incremental value.

5.5 Zeta potential measurements

The main goal of this work was the measurement of calcite surface zeta potential. While sample equilibration took up the vast majority of the time, it was only done for the sake of later performing these measurements, and the quality of the results was ultimately determined by this last step. However, in this work zeta potential measurements ended up producing highly variable results with several possible causes and implications.

The primary issue faced during measurements was the wide range of zeta potential values in almost every sample. With repeated measurements of the same cell, zeta potentials could differ by as much as ± 10 mV even if measured mere minutes apart. In some cases, both positive and negative values were recorded for the same sample in the same run. In addition, zeta potentials had a tendency to steadily increase in magnitude as more measurements were performed until appearing to settle and fluctuate around a certain value. All of this combined made it necessary to perform numerous repeat runs for every sample. Even then, data analysis remained problematic as there was no way to know which results were close to the true value and which were clear anomalies or errors. It was ultimately decided to obtain as many data points for each sample as possible to determine which values appeared most often and were the closest to one another, after which their average would be calculated and considered the “true” value. The results shown in this work were all processed in this way. However, this simple approach ignored many data points that were too far from this average as outliers, which could underestimate the uncertainty of the results. As such, the zeta potentials obtained in this work likely have a larger error associated with them than what could be accounted for and should be viewed more as indicators of trends and not as concrete values.

It is difficult to state what the cause of this large uncertainty could be. Instrument performance was likely a major factor: results from the same sample cells could differ drastically even if measured consecutively and over a short period of time, which is unlikely to have been caused by anything other the device itself. Sample preparation would have had an effect as well. Zetasizer cells are troublesome to fill, and it is likely there were differences and defects between samples, such as variations in volume and small air bubbles going unnoticed. In addition, it is worth recalling that the Zetasizer’s operation is based on the movement of charged particles, and sample aliquots consisted

of very small volumes taken from recently centrifuged solutions. As such, the number of suspended calcite particles transferred to the cells may have occasionally been so small that errors and inconsistencies in their behavior influenced the results as much as their "true" behavior. Lastly, all the issues mentioned in the previous sections would certainly have an effect as well. Prior to zeta potential measurements, all samples had to undergo equilibration, which had numerous flaws and sources of error in itself. Imperfect or incomplete equilibration would have directly affected calcite surface reactions and thus the zeta potential, and this possibility cannot be ignored due to all the issues outlined so far.

Seeing how zeta potential measurements were the last step in this work, there is little that could be improved at this stage. The preparation of samples for measurement is ultimately a matter of experience, and not much can be done about instrument performance. The biggest improvement that can be made is to address the previously mentioned issues regarding equilibration: this would likely lead to more reliable results overall, while errors arising from zeta potential measurements can simply be taken into account when discussing them. It is also worth remembering that zeta potentials are known to inherently be quite inconsistent and difficult to reproduce and compare between experimental works [32, 38]. Results are heavily dependent on numerous factors, such as electrolyte composition and concentration, the type of calcite used and its impurities, the sample preparation method, the exact experimental conditions and the measurement method itself. Slight differences in any of these factors even between samples of the same set are bound to introduce variation into the results and are difficult to keep under control.

5.6 Scope and planning

Certain issues pertaining to this work originated not from practical difficulties faced during the study, but rather its design. The lack of a well-defined scope and priorities introduced much uncertainty into the work, leading to an inefficient use of time and limiting the usefulness of the results obtained.

First, there was a lack of a concrete plan and schedule because decisions regarding every subsequent experiment were always made live based on freshly obtained results from previous sample batches. While this approach allowed for the gradual modification and refinement of experimental procedures in real time, it also means that it is very difficult to compare most samples in this work and draw conclusions. Their conditions are simply too different to make any reliable claims, which is why it was necessary to treat different samples as belonging to different batches.

For example, after Series 1 the aliquot dilution factor for MP-AES measurements was changed from 20x to 10x, meaning that the device may have had more difficulty detecting elements in the highly diluted solutions early on in the work and underestimated the true amount of Ca present. Because of this, results from Series 1 are not fully comparable with the later series due to additional uncertainty imposed by this extra variable. In addition, external standards were not yet in use while Series 1 was being worked on, adding further uncertainty to the Ca concentration. On top of that, the use of Bukov calcite was abandoned shortly after starting the work, and some equilibration solutions like $CaCl_2$ and $MgCl_2$ were only used for a limited time and not carried over between series until the end of the study. As a result, certain comparisons and conclusions also cannot be made simply because there is no data to compare to. The exact scope, priorities and direction of this work remained uncertain until it had reached the final stages, which made it difficult to know what to focus on and plan experiments accordingly.

A lack of focus also likely delayed the work considerably. As described previously, the bubbling method was utilized to accelerate the dispersion of CO_2 into sample solutions for the purposes of equilibration. However, this method still required several days of work at minimum to produce results. This work had to be done in regular intervals, in some cases daily, in order to keep sample conditions as similar as possible and make the results comparable. Bubbling had to be conducted for the same number of days and for the same length of time, and aliquots needed to be taken shortly afterwards. This created a rigid schedule for sample processing, and the need for regular, uninterrupted work contrasted greatly with its uncertain goals. Each sample batch was a significant time investment that produced a large number of aliquots, and the experiment could not be interrupted once started: as a result, it was necessary to finish all preparations before committing. Missing even one day of bubbling on any given week due to, for instance, lacking washed and labeled sample tubes for aliquots, could invalidate that entire week if there were not enough days left to finish the experiment in full, making it necessary to delay all work. The experiment setup, while simple in nature, demanded considerable preparation and was extremely sensitive to changes, requiring a clear plan and schedule for the work to be executed effectively. However, because it was sometimes not even known what the next sample batch or experiment length is going to be, it was often impossible to make preparations in advance or quickly react to new information due to the scale of the preparations. As a result, this work suffered from a considerable amount of dead time during which nothing could be done even with an otherwise clear schedule.

A lack of focus also shows in the number of variables present in this work. Every sample batch took considerable time to equilibrate and measure, with the addition of even one more meaning at least another week of work. In the case of Series 3 that lasted for a month, the effect of changes and additions would be even more severe. Because of this, it would be particularly important to carefully select what kinds of samples to investigate as any additional data would come with a large cost in time to both acquire and analyze. However, the samples used in this work varied considerably from one another: different types of calcite were equilibrated for different lengths of time in different solutions at different pH values. All of this means that, despite this work covering a fairly wide assortment of samples, only a few useful comparisons can actually be made. For instance, nothing definite can be concluded from looking at two samples of the same type of calcite that were equilibrated for a week, but at different pH values and submerged in different solutions. Investigating any one kind of sample or variable in greater detail was not possible in these conditions as there were simply too many of them and it would take too much time to study them equally. As such, while this work offers an overview of many different samples and conditions, it remains fairly shallow as no single sample batch could be investigated thoroughly. More attention was given to pure calcite in SGW2 and NaCl solutions, but even this remains quite limited in scope due to all the other work that needed to be done.

Lastly, the considerable length of each experiment and the number of experiments to perform in the available timeframe negatively affected the accuracy and reliability of the results. Because of the scale and resource-intensive nature of the work, it would have taken an unrealistic amount of time and effort to repeat any of the experiments. Parallel samples also could not be taken as even the storage and processing of primary samples already proved challenging due to the sheer quantity of them. As a result, each data point in this work is limited to only a single measurement and thus highly vulnerable to errors. In the case of CEC, this led to very high uncertainties and the need to estimate detection limits when some results proved unworkable instead of conducting further measurements to obtain more data. Furthermore, elements other than Ca were measured with MP-AES as well to obtain a clearer picture of the equilibration process, but due to time constraints and uncertainties about work priorities, external standards were never implemented for them. For this reason, despite taking considerable time to produce, results from other elements could not be processed and corrected in the same way as Ca, and thus could not be used or presented alongside Ca due to the inherent differences in reliability.

Overall, a clear goal and work plan would have been highly beneficial. This work both covers a decent assortment of different samples and investigates a few of them in greater detail, but it does not commit to either approach, which limits the quality and usefulness of the results. Very few conclusions can be drawn from wildly different samples that were also not studied for very long, while only vague trends can be speculated about with samples that received greater, but still insufficient attention. This work may serve well enough as an overview, but any future research would benefit from a more focused approach that concentrates on just one variable at a time and does not change its operating procedures during the process.

6. Conclusion

Calcite is a ubiquitous and highly reactive mineral with complicated surface chemistry. Its role as a contaminant sink as well as its many engineering applications and environmental significance make it important to understand the behavior and interactions of calcite with its environment. Because of this, considerable effort is being put into developing surface complexation models for calcite, which could aid in understanding its surface chemistry and predicting its behavior under different conditions [39, 46]. Robust and detailed models would be of great benefit to such applications as spent nuclear fuel disposal, where decisions could have considerable long-term implications, and the results presented here can further the development of such models. In this work, the zeta potentials of pure and Bukov calcite samples were investigated between pH 6.5 – 11 following a period of equilibration with CO_2 gas through direct bubbling. While numerous improvements can still be made to the procedure, this equilibration method appears to function reasonably well overall and achieves its full effect after only 3-5 days of regular 1-h bubbling sessions on average. Zeta potentials obtained from solutions equilibrated in this way repeatedly demonstrated a trend towards more negative values as the solution pH rises, which is in good agreement with theory and could thus justify further investigation and refinement of this method.

Bukov calcite did not seem to equilibrate in this work. The concentration of Ca in all samples containing Bukov calcite never stabilized and kept fluctuating even after several days of equilibration. This suggests that the number of potential-determining ions in solution remained unstable, and in these conditions zeta potentials cannot be measured reliably. For this reason Bukov calcite was not investigated further in this work, but there does not seem to be a strong theoretical basis for claiming it is incapable of equilibrating. As hinted at by its larger CEC, Bukov calcite is a

more complicated material than pure calcite and may simply require more time to stabilize. In the future, the length of the equilibration period could be increased to determine if the Ca concentration eventually achieves equilibrium. Should this not happen, it is likely that either the bubbling method is not suitable for Bukov calcite, or the presence of CO_2 overall is best avoided.

The equilibration of pure calcite met with more success. In every equilibration solution tested, the concentration of Ca quickly stabilized and did not experience any major fluctuations afterwards. Deviations from this trend were only observed below pH ≈ 8, where calcite dissolution likely begins to occur to an increasingly greater extent as pH decreases and renders equilibrium effectively impossible to achieve. On the other hand, zeta potentials for pure calcite showed considerable variation depending on the equilibration solution. The clearest and most stable trends were established using NaCl and SGW2: in every case the zeta potential steadily decreased as pH increased. In solutions containing $MgCl_2$ the zeta potentials did not appear to correlate with anything: all data points are scattered randomly, likely due to the interfering presence of Mg^{2+} as an additional potential-determining ion. Overall, the bubbling method appears to function well for equilibrating pure calcite and does not require more than 3-5 days to achieve its full effect. Ca concentration stabilizes quite quickly during the initial few days, and no disturbances or improvements to stability were noted to occur even after one additional month of equilibration in the case of NaCl and SGW2. The effect of a longer equilibration time on zeta potential is not as clear, however. No significant difference was observed with pure calcite in SGW2 after continuing equilibration for a month after the initial 5 days, but results for pure calcite in NaCl seemed to improve after the same procedure. In the future, more equilibrations could be conducted in the short and long term to gather more data and come to a more definite conclusion.

Equilibration with CO_2 may lead to more stable sample conditions and improve the reliability of zeta potential results, but more experiments should be conducted to obtain more reliable data. The bubbling setup utilized in this work suffered from many design flaws that increased uncertainty, and it was not possible to conduct repeat measurements or investigate samples in detail given the time constraints. Addressing the issues outlined in Section 5 would be critical to any future investigations. In addition, it is worth noting that Ca concentration may not be sufficient to track the progress of equilibration by itself. Equilibration as defined in this work technically was reliably achieved in all cases, but this did not always translate to good-quality zeta potential results. This is most clearly seen in NaCl/$MgCl_2$ solutions: their concentrations of Ca remained just as stable over time as in all

other solutions, but due to the presence of Mg^{2+}, their zeta potential results are essentially a random spread of values. As such, the procedure described in this work does not account for the presence of contaminants, competing potential-determining ions and the effect of any other factors, which should be noted when evaluating zeta potential results.

7. References

1. Hedin A (1997) Spent nuclear fuel - how dangerous is it? A report from the project "Description of risk"

2. (2012) Safety case for the disposal of spent nuclear fuel at Olkiluoto. Complementary considerations 2012. Posiva Oy, Olkiluoto

3. Neall F, Pastina B, Snellman M, et al Safety assessment of a KBS-3H spent nuclear fuel repository at Olkiluoto - Complementary evaluations of safety

4. (2012) Safety case for the disposal of spent nuclear fuel at Olkiluoto. Synthesis 2012. Posiva Oy, Olkiluoto

5. (2012) Safety case for the disposal of spent nuclear fuel at Olkiluoto. Description of the disposal system 2012. Posiva Oy, Olkiluoto

6. Hakanen M, Ervanne H, Puukko E (2014) Safety case for the disposal of spent nuclear fuel at Olkiluoto. Radionuclide migration parameters for the geosphere. Posiva Oy, Olkiluoto

7. Lakshtanov LZ, Stipp SLS (2007) Experimental study of nickel(II) interaction with calcite: Adsorption and coprecipitation. Geochimica et Cosmochimica Acta 71:3686–3697. https://doi.org/10.1016/j.gca.2007.04.006

8. Zavarin M, Roberts SK, Hakem N, et al (2005) Eu(III), Sm(III), Np(V), Pu(V), and Pu(IV) sorption to calcite. Radiochimica Acta 93:93–102. https://doi.org/10.1524/ract.93.2.93.59413

9. Heberling F, Brendebach B, Bosbach D (2008) Neptunium(V) adsorption to calcite. Journal of Contaminant Hydrology 102:246–252. https://doi.org/10.1016/j.jconhyd.2008.09.015

10. Heberling F, Denecke MA, Bosbach D (2008) Neptunium(V) Coprecipitation with Calcite. Environ Sci Technol 42:471–476. https://doi.org/10.1021/es071790g

11. Stumpf T, Fanghänel T (2002) A Time-Resolved Laser Fluorescence Spectroscopy (TRLFS) Study of the Interaction of Trivalent Actinides (Cm(III)) with Calcite. Journal of Colloid and Interface Science 249:119–122. https://doi.org/10.1006/jcis.2002.8251

12. Geipel G, Reich T, Brendler V, et al (1997) Laser and X-ray spectroscopic studies of uranium-calcite interface phenomena. Journal of Nuclear Materials 248:408–411. https://doi.org/10.1016/S0022-3115(97)00136-0

13. Reeder RJ, Nugent M, Lamble GM, et al (2000) Uranyl Incorporation into Calcite and Aragonite: XAFS and Luminescence Studies. Environ Sci Technol 34:638–644. https://doi.org/10.1021/es990981j

14. Curti E (1999) Coprecipitation of radionuclides with calcite: estimation of partition coe□cients based on a review of laboratory investigations and geochemical data. Applied Geochemistry

15. Villegas-Jiménez A, Mucci A, Paquette J (2009) Proton/calcium ion exchange behavior of calcite. Phys Chem Chem Phys 11:8895. https://doi.org/10.1039/b815198a

16. Hazen RM, Downs RT, Jones AP, Kah L (2013) Carbon Mineralogy and Crystal Chemistry. Reviews in Mineralogy and Geochemistry 75:7–46. https://doi.org/10.2138/rmg.2013.75.2

17. James NP (2015) Origin of Carbonate Sedimentary Rocks. American Geophysical Union, Newark, UNITED STATES

18. Heberling F, Trainor TP, Lützenkirchen J, et al (2011) Structure and reactivity of the calcite–water interface. Journal of Colloid and Interface Science 354:843–857. https://doi.org/10.1016/j.jcis.2010.10.047

19. Hazen RM, Downs RT, Kah L, Sverjensky D (2013) Carbon Mineral Evolution. Reviews in Mineralogy and Geochemistry 75:79–107. https://doi.org/10.2138/rmg.2013.75.4

20. Hazen RM, Papineau D, Bleeker W, et al (2008) Mineral evolution. American Mineralogist 93:1693–1720. https://doi.org/10.2138/am.2008.2955

21. Knoll AH (2003) Biomineralization and Evolutionary History. Reviews in Mineralogy and Geochemistry 54:329–356. https://doi.org/10.2113/0540329

22. Alderton D (2021) Carbonates (Ca, Mg, Fe, Mn). In: Encyclopedia of Geology. Elsevier, pp 382–394

23. Smyth JR, Ahrens TJ (1997) The crystal structure of calcite III. Geophys Res Lett 24:1595–1598. https://doi.org/10.1029/97GL01603

24. Tertre E, Beaucaire C, Juery A, Ly J (2010) Methodology to obtain exchange properties of the calcite surface—Application to major and trace elements: Ca(II), , and Zn(II). Journal of Colloid and Interface Science 347:120–126. https://doi.org/10.1016/j.jcis.2010.03.040

25. Tesoriero AJ, Pankow JF (1996) Solid solution partitioning of Sr2+, Ba2+, and Cd2+ to calcite. Geochimica et Cosmochimica Acta 60:1053–1063. https://doi.org/10.1016/0016-7037(95)00449-1

26. Belova DA, Lakshtanov LZ, Carneiro JF, Stipp SLS (2014) Nickel adsorption on chalk and calcite. Journal of Contaminant Hydrology 170:1–9. https://doi.org/10.1016/j.jconhyd.2014.09.007

27. Jones MJ, Butchins LJ, Charnock JM, et al (2011) Reactions of radium and barium with the surfaces of carbonate minerals. Applied Geochemistry 26:1231–1238. https://doi.org/10.1016/j.apgeochem.2011.04.012

28. Martin-Garin A, Van Cappellen † P., Charlet L (2003) Aqueous cadmium uptake by calcite: a stirred flow-through reactor study. Geochimica et Cosmochimica Acta 67:2763–2774. https://doi.org/10.1016/S0016-7037(03)00091-7

29. Pokrovsky OS, Pokrovski GS, Schott J (2004) Gallium(III) adsorption on carbonates and oxides: X-ray absorption fine structure spectroscopy study and surface complexation modeling. Journal of Colloid and Interface Science 279:314–325. https://doi.org/10.1016/j.jcis.2004.06.095

30. Bukov U (2017) The Bukov Underground Research Facility. https://www.pvpbukov.cz/en/about-urf/. Accessed 24 Aug 2023

31. Dohrmann R, Kaufhold S (2009) Three New, Quick CEC Methods for Determining the Amounts of Exchangeable Calcium Cations in Calcareous Clays. Clays Clay Miner 57:338–352. https://doi.org/10.1346/CCMN.2009.0570306

32. The Zeta Potential for Solid Surface Analysis - A practical guide to streaming potential measurement | Web-Books in the Austria-Forum. https://austria-forum.org/web-books/en/zeta00en2014iicm. Accessed 21 Aug 2023

33. Stricker A (2021) Characterisation of the calcite-groundwater interface: cation exchange capacity and zeta potential measurements with the streaming potential method. University of Leipzig

34. (2007) Zetasizer Nano User Manual MAN0317

35. Vdović N (2001) Electrokinetic behaviour of calcite—the relationship with other calcite properties. Chemical Geology 177:241–248. https://doi.org/10.1016/S0009-2541(00)00397-1

36. Van Cappellen P, Charlet L, Stumm W, Wersin P (1993) A surface complexation model of the carbonate mineral-aqueous solution interface. Geochimica et Cosmochimica Acta 57:3505–3518. https://doi.org/10.1016/0016-7037(93)90135-J

37. Stipp SLS (1999) Toward a conceptual model of the calcite surface: hydration, hydrolysis, and surface potential. Geochimica et Cosmochimica Acta 63:3121–3131. https://doi.org/10.1016/S0016-7037(99)00239-2

38. Al Mahrouqi D, Vinogradov J, Jackson MD (2017) Zeta potential of artificial and natural calcite in aqueous solution. Advances in Colloid and Interface Science 240:60–76. https://doi.org/10.1016/j.cis.2016.12.006

39. Tertre E, Page J, Beaucaire C (2012) Ion Exchange Model for Reversible Sorption of Divalent Metals on Calcite: Implications for Natural Environments. Environ Sci Technol 46:10055–10062. https://doi.org/10.1021/es301535g

40. Vdović N, Bisćan J (1998) Electrokinetics of natural and synthetic calcite suspensions. Colloids Surfaces A: Physicochem Eng Aspects 137:7–14

41. Vysetti B (2014) Analysis of Geochemical Samples by Microwave Plasma-AES. AtSpectrosc 35:154–162. https://doi.org/10.46770/AS.2014.02.003

42. Niedzielski P, Kozak L, Wachelka M, et al (2015) The microwave induced plasma with optical emission spectrometry (MIP–OES) in 23 elements determination in geological samples. Talanta 132:591–599. https://doi.org/10.1016/j.talanta.2014.10.009

43. Balaram V (2020) Microwave plasma atomic emission spectrometry (MP-AES) and its applications – A critical review. Microchemical Journal 159:105483. https://doi.org/10.1016/j.microc.2020.105483

44. Hammer MR (2008) A magnetically excited microwave plasma source for atomic emission spectroscopy with performance approaching that of the inductively coupled plasma. Spectrochimica Acta Part B: Atomic Spectroscopy 63:456–464. https://doi.org/10.1016/j.sab.2007.12.007

45. Jaremko D, Kalembasa D (2014) A Comparison of Methods for the Determination of Cation Exchange Capacity of Soils/Porównanie Metod Oznaczania Pojemności Wymiany Kationów I Sumy Kationów Wymiennych W Glebach. Ecological Chemistry and Engineering S 21:487–498. https://doi.org/10.2478/eces-2014-0036

46. Sameh EF (2011) Sorption of Ni and Eu to Granitic Rocks and Minerals. Loughborough University

47. Dohrmann R (2006) Cation exchange capacity methodology III: Correct exchangeable calcium determination of calcareous clays using a new silver–thiourea method. Applied Clay Science 34:47–57. https://doi.org/10.1016/j.clay.2006.02.010

48. Dohrmann R (2006) Problems in CEC determination of calcareous clayey sediments using the ammonium acetate method. Z Pflanzenernähr Bodenk 169:330–334. https://doi.org/10.1002/jpln.200621975

49. Ciesielski H, Sterckeman T, Santerne M, Willery JP (1997) Determination of cation exchange capacity and exchangeable cations in soils by means of cobalt hexamine trichloride. Effects of experimental conditions. Agronomie 17:1–7. https://doi.org/10.1051/agro:19970101

50. Näykki T, Magnusson B, Helm I, et al (2014) Comparison of measurement uncertainty estimates using quality control and validation data. J Chem Metrol

51. Magnusson B, Ab T, Näykki T, et al (2017) Handbook for calculation of measurement uncertainty in environmental laboratories

52. Knoll GF (2010) Radiation detection and measurement, 4th ed. John Wiley, Hoboken, N.J

53. Zachara JM, Cowan CE, Resch CT (1991) Sorption of divalent metals on calcite. Geochimica et Cosmochimica Acta 55:1549–1562. https://doi.org/10.1016/0016-7037(91)90127-Q

54. Song J, Zeng Y, Wang L, et al (2017) Surface complexation modeling of calcite zeta potential measurements in brines with mixed potential determining ions (Ca2+, CO32−, Mg2+, SO42−) for characterizing carbonate wettability. Journal of Colloid and Interface Science 506:169–179. https://doi.org/10.1016/j.jcis.2017.06.096

55. Astilleros JM, Fernández-Díaz L, Putnis A (2010) The role of magnesium in the growth of calcite: An AFM study. Chemical Geology 271:52–58. https://doi.org/10.1016/j.chemgeo.2009.12.011

56. Zhang Y, Dawe RA (2000) Influence of Mg2+ on the kinetics of calcite precipitation and calcite crystal morphology. Chemical Geology 163:129–138. https://doi.org/10.1016/S0009-2541(99)00097-2

57. De Choudens-Sanchez V, Gonzalez LA (2009) Calcite and Aragonite Precipitation Under Controlled Instantaneous Supersaturation: Elucidating the Role of CaCO3 Saturation State and Mg/Ca Ratio on Calcium Carbonate Polymorphism. Journal of Sedimentary Research 79:363–376. https://doi.org/10.2110/jsr.2009.043

58. Abdollahpour M, Heberling F, Schild D, Rahnemaie R (2022) Magnesium Coprecipitation with Calcite at Low Supersaturation: Implications for Mg-Enriched Water in Calcareous Soils. Minerals 12:265. https://doi.org/10.3390/min12020265

59. Shannon RD (1976) Revised effective ionic radii and systematic studies of interatomic distances in halides and chalcogenides. Acta Crystallographica Section A 32:751–767. https://doi.org/10.1107/S0567739476001551

60. Pierre A, Lamarche JM, Mercier R, et al (1990) CALCIUM AS POTENTIAL DETERMINING ION IN AQUEOUS CALCITE SUSPENSIONS. Journal of Dispersion Science and Technology 11:611–635. https://doi.org/10.1080/01932699008943286